Article
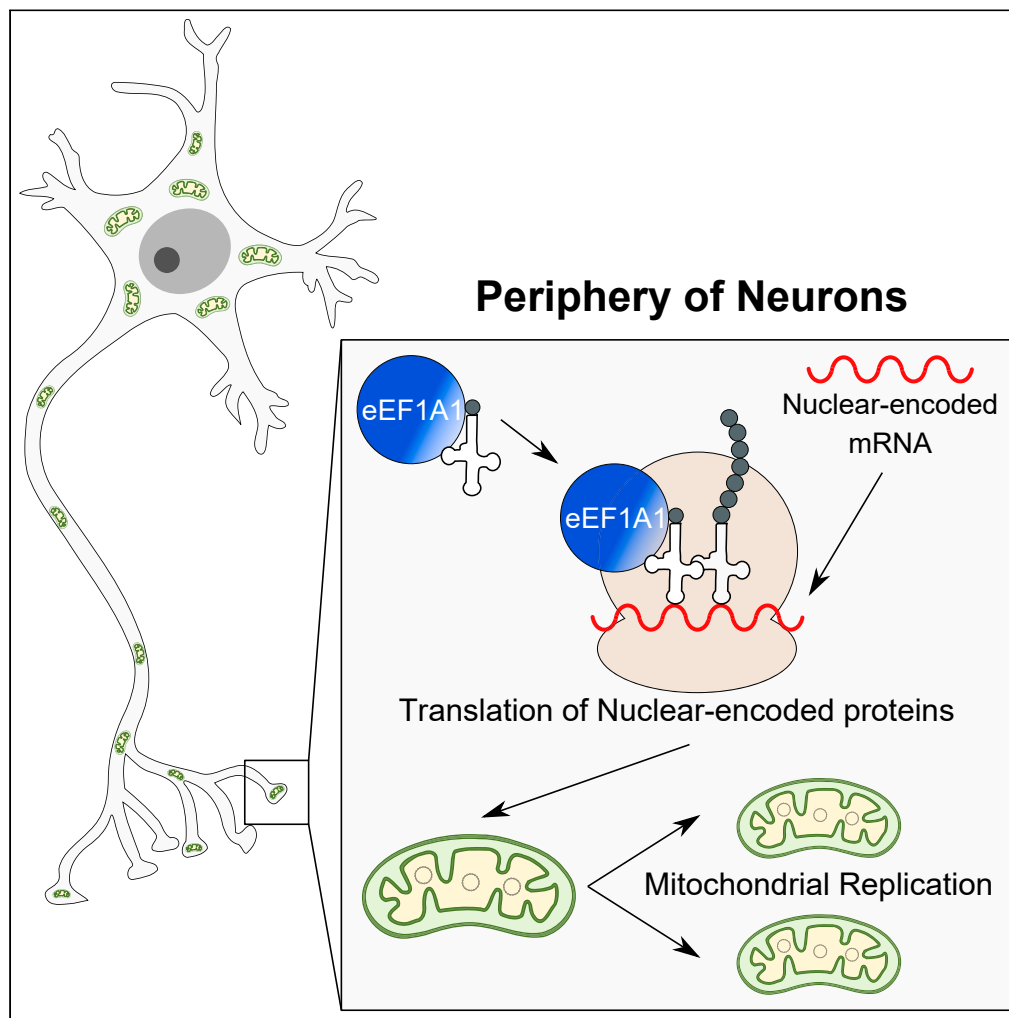
Local mitochondrial replication in the periphery of neurons requires the eEF1A1 protein and thetranslation of nuclear-encoded proteins

Periphery of Neurons

eEF1A1

eEF1A1

Nuclear-encoded mRNA

Translation of Nuclear-encoded proteins

Mitochondrial Replication

Carlos Cardanho-Ramos, Rúben Alves Simões, Yi-Zhi Wang, ..., Marco Spinazzi, Jeffrey N. Savas, Vanessa A. Morais

vmorais@medicina.ulisboa.pt

Highlights

Mitochondrial replication occurs in distal regions of neurons

Mitochondrial-encoded translation is not required for mtDNA replication in neurons

In neurons, mitochondrial replication requires nuclear-encoded protein translation

EEF1A1 is upregulated at the synapse and is required for mitochondrial replication

Article

Local mitochondrial replication in the periphery of neurons requires the eEF1A1 protein and the translation of nuclear-encoded proteins

Carlos Cardanho-Ramos,[1] Rúben Alves Simões,[1] Yi-Zhi Wang,[2] Andreia Faria-Pereira,[1] Ewa Bomba-Warczak,[2] Katleen Craessaerts,[3,4] Marco Spinazzi,[3,4,5] Jeffrey N. Savas,[2] and Vanessa A. Morais[1,6,*]

SUMMARY

In neurons, it is commonly assumed that mitochondrial replication only occurs in the cell body, after which the mitochondria must travel to the neuron's periphery. However, while mitochondrial DNA replication has been observed to occur away from the cell body, the specific mechanisms involved remain elusive. Using EdU-labelling in mouse primary neurons, we developed a tool to determine the mitochondrial replication rate. Taking of advantage of microfluidic devices, we confirmed that mitochondrial replication also occurs locally in the periphery of neurons. To achieve this, mitochondria require *de novo* nuclear-encoded, but not mitochondrial-encoded protein translation. Following a proteomic screen comparing synaptic with non-synaptic mitochondria, we identified two elongation factors – eEF1A1 and TUFM – that were up-regulated in synaptic mitochondria. We found that mitochondrial replication is impaired upon the down-regulation of eEF1A1, and this is particularly relevant in the periphery of neurons.

INTRODUCTION

Neurons are high energy demanding cells that rely on mitochondria not only for ATP production, but also to maintain a tight regulation of Ca^{2+}. Neurons have complex morphologies and are composed of different sub-compartments, namely the cell body, dendrites, and axons. Each compartment has its own unique function and requires a specific pool of mitochondria.[1–3] To achieve this, mitochondria are transported, they fuse, divide, and undergo a selective autophagy process named mitophagy.[4,5] Although all these processes are important, maintaining a healthy pool of mitochondria within neurons is only possible due to mitochondrial biogenesis. Mitochondrial biogenesis is a set of molecular processes that include mitochondrial DNA (mtDNA) replication and ultimately results in the formation of new mitochondria. mtDNA encodes for 13 proteins, whereas the remaining over 1000 mitochondrial proteins are nuclear-encoded.[6] Thus, it comes as no surprise that the canonical pathway of mitochondrial replication involves the activation of nuclear transcription. This is achieved by the master regulator of mitochondrial biogenesis, the peroxisome-proliferator-activated γ co-activator-1α (PGC-1α). PGC-1α is a co-activator of transcription that binds to the nuclear respiratory factors 1 and 2 (NRF-1 and NRF-2), leading to the transcription of several mitochondrial genes, including proteins involved in mtDNA replication, such as the mitochondrial transcription factor A (TFAM).[7–9] Increasing evidence has shown that PGC-1α, NRF-1 and TFAM are downregulated in several neurodegenerative diseases, such as Huntington's,[10,11] Parkinson's[12–14] and Alzheimer's diseases.[15,16] This is accompanied by a decrease in mitochondrial content,[14,16,17] suggesting that deficits in mitochondrial replication are associated with neurodegeneration.

In neurons, it is generally assumed that mitochondria replicate in the cell body and then have to travel all the way to the neuron's periphery.[18–20] However, considering that the rate of mitochondrial transport in mouse neurons is about 0.6μm/s,[21] the time it would take for a single mitochondrion to travel from the cell body to the tip of an axon exceeds the half-life of most mitochondrial proteins.[22] Although mitochondrial replication has been observed away from the cell body,[23,24] very little is known about the mechanisms involved, making the question of whether or not mitochondria are capable of replicating locally in distal regions of neurons still controversial. Since renewal of mitochondria requires *de novo* transcription mediated by the nuclear proteins PGC-1α and NRF-1/2, distal mitochondria must have an alternative mechanism to have access to all the proteins necessary for mitochondrial replication. Interestingly, mRNAs are present in distal regions of neurons.[25,26] These mRNAs have longer 3′ untranslated regions (UTRs), making them more stable and with longer half-lives, when compared to mRNAs present in the cell body.[27] Moreover, the translation of both mitochondrial-[28] and nuclear-encoded[29,30] proteins have been

[1]Instituto de Medicina Molecular-João Lobo Antunes, Faculdade de Medicina, Universidade de Lisboa, Lisboa, Portugal
[2]Department of Neurology, Northwestern University Feinberg School of Medicine, Chicago, IL 60611, USA
[3]VIB Center for Brain and Disease Research and KU Leuven, Department of Neurosciences, Leuven, Belgium
[4]Dementia Research Institute, University College London, London, UK
[5]Neuromuscular Reference Center, Department of Neurology, Centre Hospitalier Universitaire d'Angers, Angers, France
[6]Lead contact
*Correspondence: vmorais@medicina.ulisboa.pt
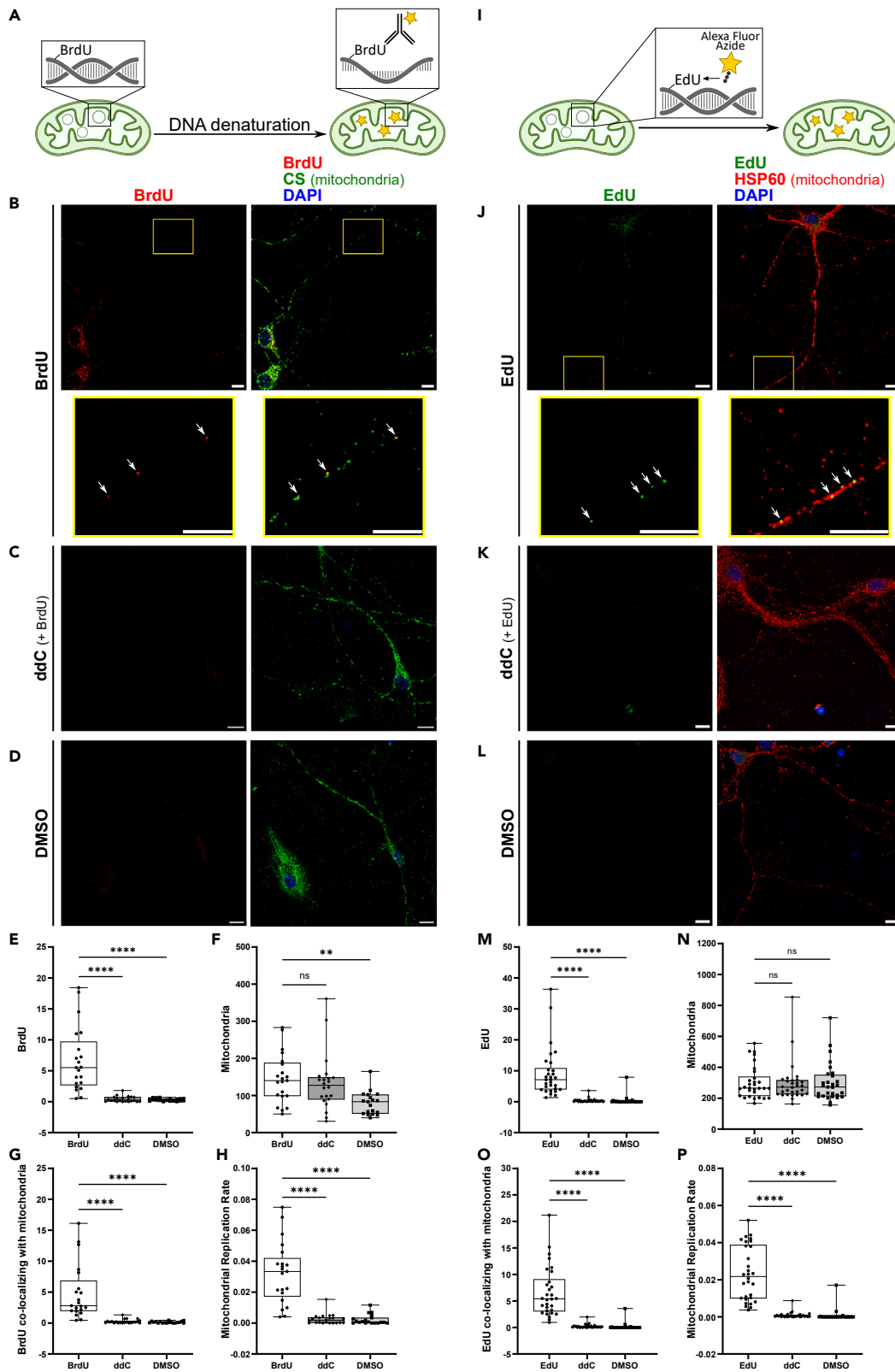https://doi.org/10.1016/j.isci.2024.109136

Figure 1. BrdU and EdU can be used to determine mitochondrial replication in mouse primary neurons

(A) Representative scheme of the BrdU protocol that requires a DNA denaturation step.

(B–D) Representative images of mouse primary neurons stained for BrdU, in red, and citrate synthase (CS, mitochondrial marker), in green. Neurons were incubated with BrdU (B); an inhibitor of mtDNA replication, ddC (+BrdU), (C); and DMSO (no BrdU) (D). Arrows indicate sites of mitochondrial replication in the periphery of neurons. Scale bar 10μm.

(E–H) Quantification of the Area for BrdU (E); Mitochondria (F); and BrdU co-localizing with Mitochondria (G). For each image, mitochondrial replication rate was determined by dividing the area of BrdU co-localizing with mitochondria by the area of mitochondria (H). n = 19–22 neurons, from 3 independent experiments.

(I) Representative scheme of the EdU click chemistry protocol.

(J–L) Representative images of mouse primary neurons stained for EdU, in green, and HSP60 (mitochondrial marker), in red. Neurons were incubated with EdU (J); an inhibitor of mtDNA replication, ddC (+EdU), (K); and DMSO (no EdU) (L). Arrows indicate sites of mitochondrial replication in the periphery of neurons. Scale bar 10μm.

(M–P) Quantification of the Area for EdU (M); Mitochondria (N); and EdU co-localizing with Mitochondria (O). For each image, mitochondrial replication rate was determined by dividing the area of EdU co-localizing with mitochondria by the area of mitochondria (P). n = 29–30 neurons, from 3 independent experiments. One-way ANOVA with a Dunnet multiple comparison test (EdU as the control). ns = non-significant; **p < 0.01; ****p < 0.0001. Related to Figure S1.

observed in axons. These data led us to speculate that mRNAs, which can be translated several times, are present in the distal regions of neurons, providing all the proteins necessary for local mitochondrial replication.

Here, we confirm that mitochondrial replication occurs in the periphery of neurons. We observe that his is achieved by local nuclear-encoded protein translation, in a process involving the eukaryotic translation elongation factor 1 alpha 1 (eEF1A1).

RESULTS

Assessment of mitochondrial replication in mouse primary neurons using 5′-bromo-2′-deoxyuridine - and 5-ethyl-2′-deoxyuridine labelling

To determine the specific localization of mtDNA replication within mouse primary neurons, we used 5′-bromo-2′-deoxyuridine (BrdU) and 5-ethynyl-2′-deoxyuridine (EdU). These two nucleosides are analogues of thymidine and are incorporated into DNA during active DNA replication.[23,24] Since neurons are post-mitotic cells, BrdU and EdU will only be incorporated into replicating mtDNA. Neurons were incubated with 10μM BrdU for 4h and, after fixation, a DNA denaturing step was performed using 1M HCl, exposing the BrdU epitope for consequent anti-BrdU antibody recognition (Figure 1A). By co-staining with the mitochondrial marker citrate synthase (CS), we were able to determine the mitochondrial replication rate. As expected, most BrdU was observed in the somal region of neurons (Figure 1B). Nonetheless, some BrdU⁺ mitochondria were also observed far away from the soma (Figure 1B), indicating that mtDNA replication can occur locally in the periphery of neurons. To validate the specificity of BrdU to mitochondrial replication sites, we co-incubated BrdU with 2′,3′-dideoxycytidine (ddC), an inhibitor of mtDNA replication. As a solvent control, we also incubated neurons only with DMSO (no BrdU). No signal for BrdU was observed in neither ddC (Figure 1C), nor DMSO (Figure 1D). This was confirmed by the significantly higher levels of BrdU (Figure 1E), BrdU co-localizing with mitochondria (Figure 1G) and mitochondrial replication rate (Figure 1H), when neurons were incubated with BrdU alone. Although we confirmed the BrdU signal was specific for mitochondrial replication sites, the DNA denaturation step required in this protocol is too harsh for the cells, as it alters the morphology of neurons, particularly at the level of the mitochondrial network. Mitochondria exposed to the DNA denaturation step appear more punctated (Figure S1) and this could have an impact on the quantification of the mitochondrial replication rate. To overcome this, we took advantage of EdU click chemistry. In this case, detection is based on a copper-catalyzed covalent reaction between the alkyne group present in EdU and an Alexa Fluorophore-conjugated Azide[31] (Figure 1I). Similar to the BrdU approach, neurons were treated with EdU, ddC (+EdU), and DMSO. No EdU staining was observed in neither ddC (Figures 1K and 1M) nor DMSO (Figures 1L and 1M), as confirmed by the significantly higher mitochondrial replication rate in neurons incubated with EdU alone (Figure 1P). We validated that EdU click chemistry can also be used to assess mitochondrial replication in mouse primary neurons. By avoiding the DNA denaturation step, we are able to quantify the mitochondrial replication rate in a more reliable manner, making EdU a better alternative when compared to BrdU.

Mitochondrial replication occurs locally in the periphery of neurons

We observed BrdU⁺ and EdU⁺ mitochondria in the periphery of neurons, however, we were unable to discriminate if those mitochondria replicated in the cell body and were transported to the periphery or if they replicated locally at the periphery of the neuron. To answer this question, we cultured mouse primary neurons in microfluidic devices, where we can isolate axons from the soma and dendrites.[32] These devices have two distinct compartments, separated by microgrooves that only allow axons to reach the axonal side. Neurons were plated in the somal compartment, and after 8 days *in vitro* (DIV8), we observed the presence of β3-tubulin⁺ axons, but not MAP2⁺ dendrites, in the axonal compartment (Figure 2A). This allowed us to perform chemical treatments only to the axonal compartment, without interfering with the somal side. We incubated axons with EdU; ddC (+EdU) or DMSO and then stained both compartments for EdU and the mitochondrial marker HSP60 (Figure 2B). EdU puncta and EdU⁺ mitochondria were mostly present in axons incubated with EdU only (Figures 2C and 2D). This observation was corroborated by the statistically significant mitochondrial replication rate observed in EdU when compared to ddC and DMSO (Figure 2F). To confirm these results were specific for axons, we also analyzed the somal compartments of EdU (Figure 2E), ddC (Figure S2F), and DMSO (Figure S2E). No differences were observed in the somal compartments, neither
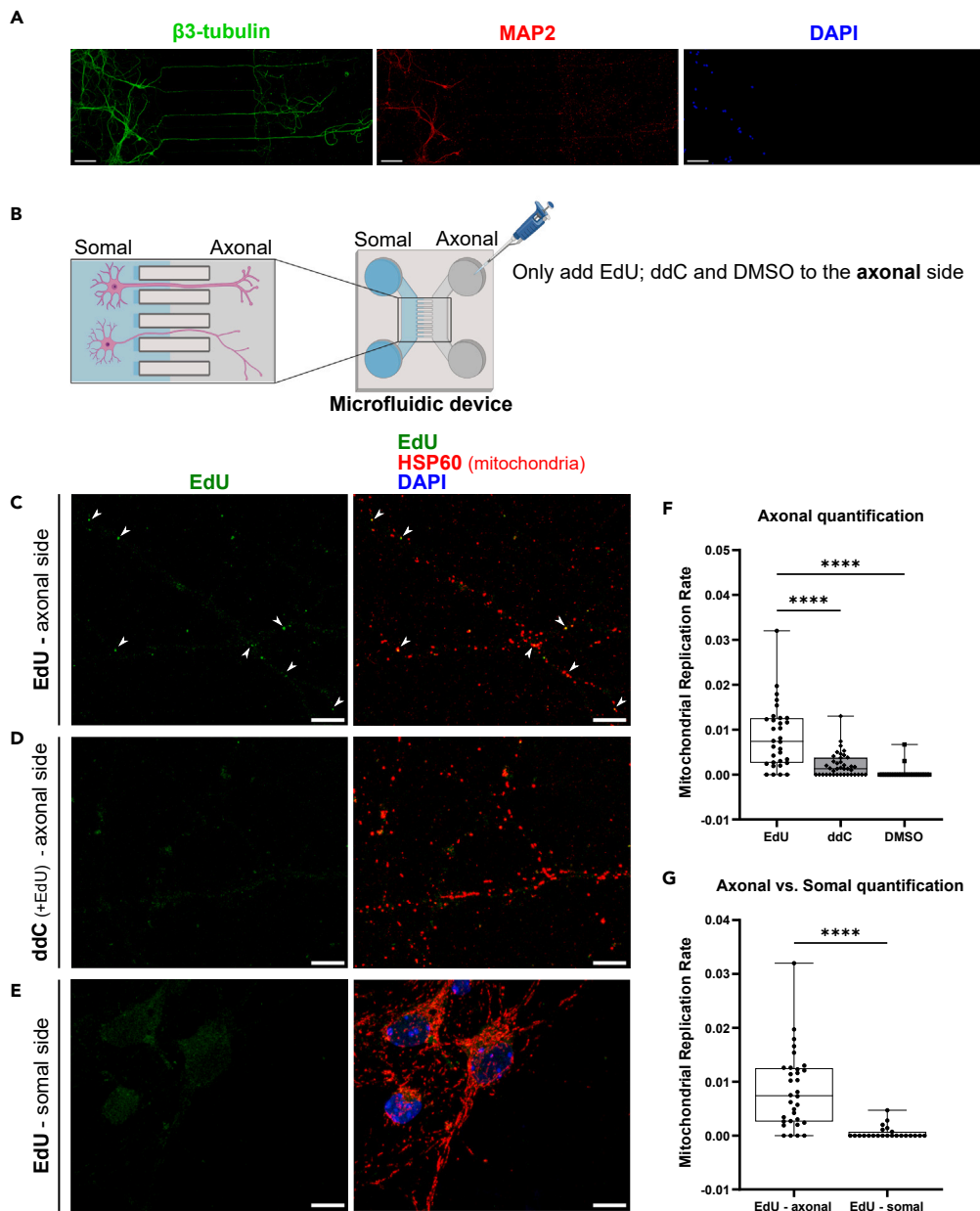
Figure 2. Mitochondrial replication in neurons can occur locally, away from the cell body

(A) Validation of microfluidics devices. At DIV8, only axons reach the axonal side, as observed by the presence of β3-tubulin staining, but not MAP2 (dendritic marker) or DAPI (nuclei). Scale bar 100μm.

(B) Scheme of the experimental design in microfluidic devices.

(C–E) Representative images stained of the axonal side in EdU (C) and ddC (+EdU) (D) conditions; and of the somal side in EdU condition (E). EdU, in green, and HSP60 (mitochondrial marker), in red. Arrows indicate sites of mitochondrial replication. Scale bar 10μm.

(F) Quantification of the mitochondrial replication rate in the axonal side. n = 24–39 axons, from 3 independent experiments. One-way ANOVA with a Dunnet multiple comparison test (EdU as control). ****$p < 0.0001$.

(G) Quantification of the mitochondrial replication rate comparing Axonal with Somal side in EdU condition. n = 23–32 axons/neurons, from 3 independent experiments. Unpaired t test. ****$p < 0.0001$. Related to Figure S2.

at the level of EdU (Figure S2G), EdU co-localizing with mitochondria (Figure S2I), nor mitochondrial replication rate (Figure S2J). Finally, in the condition where we only add EdU to the axonal compartment, we observed a significantly higher mitochondrial replication rate in axons when compared to the soma (Figure 2G). With these results, we confirm that mitochondrial replication can occur locally in the periphery of neurons.

Mitochondrial replication in neurons requires nuclear-encoded protein translation

Within the mitochondrial biogenesis pathways described so far, mitochondrial replication requires the activation of nuclear transcription by PGC-1α and NRF-1/2[7]. Since PGC-1α and NRF-1/2 only act in the nucleus, it is unlikely that mitochondria that replicate in the periphery of neurons also rely on *de novo* nuclear transcription. Interestingly, reports have shown that mRNAs encoding for mitochondrial proteins are present in axons,[25] and that the axonal translation of both mitochondrial-[28] and nuclear-encoded[26,29,30] proteins has been observed. We hypothesized that mitochondrial replication in the periphery of neurons is sustained by local protein translation. To test this, we inhibited protein translation and assessed the impact on mitochondrial replication. Since mitochondria are composed of proteins encoded by nuclear and mitochondrial DNA, we used two different approaches. Mouse primary neurons were treated either with cycloheximide or chloramphenicol. Cycloheximide binds to cytosolic ribosomes, inhibiting nuclear-encoded protein translation.[33] This effect of cycloheximide was confirmed, using the puromycin assay as a readout of protein translation (Figure S3A). On the other hand, chloramphenicol binds to the mitochondrial ribosomal subunits, inhibiting mitochondrial-encoded protein translation. Taking advantage of L-homopropargylglycine (HPG), which incorporates translation products instead of methionine,[28] we confirmed that the pattern of HPG that co-localized with mitochondria was only sensitive to chloramphenicol and not cycloheximide (Figure S4A). Additionally, we wanted to understand if the impact of protein translation inhibition on mitochondrial replication was dependent on the maturation stage of mouse primary neurons. We treated neurons with cycloheximide and chloramphenicol either at DIV7 - where neurons are still maturating, but synapses are already present to some extent – or at DIV14 – where neurons are mature and a higher number of synapses are established.[34]

Nuclear-encoded protein translation was inhibited in mouse primary neurons with cycloheximide at different time points. We pre-incubated cycloheximide for 30min or for 4h prior to EdU; or we co-incubated cycloheximide and EdU at the same time. At DIV7, we observed a decrease in EdU puncta independently of the time of incubation of cycloheximide (Figure 3A). This was confirmed by the significantly lower levels of EdU (Figure S3C), Edu co-localizing with mitochondria (Figure S3E), and mitochondria replication rate (Figure 3B) observed in all cycloheximide time-points. At DIV14, differences in EdU puncta were only found in the conditions where cycloheximide was pre-incubated before EdU (Figures 3C and S3G). In accordance, the mitochondrial replication rate was similar when neurons were co-incubated with cycloheximide at the same time of EdU, or EdU alone (Figure 3D). Still, a significant decrease in mitochondrial replication rate was observed when neurons were pre-incubated with cycloheximide for 30min and for 4h (Figure 3D). The differences between the two stages of maturation indicate that neurons at DIV7 are more sensitive to the inhibition of nuclear-encoded protein translation. This may be explained by the observation that the mitochondrial replication rate at DIV7 is significantly higher when compared to DIV14 (Figure S3J). Nonetheless, and independently of the stage of maturation, we can conclude that, in mouse primary neurons, *de novo* nuclear-encoded protein translation is required for mitochondria to replicate.

Mitochondrial-encoded protein translation was inhibited in mouse primary neurons by pre-incubating chloramphenicol for 3h before adding EdU. At both stages of neuronal maturation, DIV7 and DIV14, we observed a significant decrease in EdU (Figures S4C and S4G) and EdU-colocalizing with mitochondria (Figures S4E and S4I) when neurons were treated with chloramphenicol. However, we also observed a significant decrease in mitochondrial area in these conditions (Figures S4D and S4H), explaining the observed decrease in EdU staining. Moreover, no differences in the mitochondrial replication rate were found between the pre-incubation of chloramphenicol for 3h and EdU alone (Figures 4B and 4D). To confirm that the inhibition of mitochondrial-encoded protein translation had no impact on mitochondrial replication, we also pre-incubated chloramphenicol overnight, prior to EdU. No differences in EdU (Figures S4C and S4G), EdU co-localizing with mitochondria (Figures S4D and S4H), and mitochondrial replication rate (Figures 4B and 4D) were observed between the pre-incubation of chloramphenicol overnight and EdU alone; neither at DIV7, nor at DIV14. Thus, mitochondrial replication in mouse primary neurons does not require *de novo* mitochondrial-encoded protein translation.

Translation elongation factors TUFM and eukaryotic translation elongation factor 1 alpha 1 are upregulated in synaptic mitochondria

Having established that mitochondrial replication in neurons requires nuclear-encoded protein synthesis, we set out to identify specifically which proteins were involved in mitochondrial replication in the periphery of neurons. For that, synaptic and non-synaptic mitochondria were isolated from mouse brains, and a label-free proteomic screen was performed (Figure 5A). As expected, an enrichment of the mitochondrial marker HSP60 was observed in both synaptic and non-synaptic mitochondria, whereas the synaptic markers, Post Synaptic Density 95 (PSD95) and Synaptophysin1 were only detected in the synaptic fraction (Figure S5A). Moreover, the Glial Fibrillary Acidic Protein (GFAP) was detected at low levels in synaptic and non-synaptic mitochondria, when compared to brain homogenate (Figure S5B), indicating reduced glial contamination in these mitochondrial fractions. ^{15}N-fed mice were used as internal standards, allowing direct comparison between the two mitochondrial fractions. Using liquid chromatography followed by tandem mass spectrometry (LC-MS/MS), we were able to identify 211 proteins that were differently expressed (Figure 5B). Of these, 195 proteins were significantly upregulated in synaptic mitochondria, while 16 proteins were significantly upregulated in non-synaptic mitochondria (Figure 5B). One of the proteins found upregulated in synaptic mitochondria was the eukaryotic elongation factor 1 alpha 1 (eEF1A1) (Figure 5C). It has been reported that, during postnatal development, eEF1A1 is replaced in neurons by its homologue eEF1A2.[35,36] These studies focus on either total protein levels in the brain or localization in the neuronal soma. In our data, eEF1A2 was identified as being similarly expressed in both pools of mitochondria (Figure 5B), indicating that the upregulation of eEF1A1 is specific to synaptic mitochondria. This is in line with recent studies, where eEF1A1 is present in postnatal neurons and is found upregulated in axons, both at the mRNA[37] and protein[38] levels.
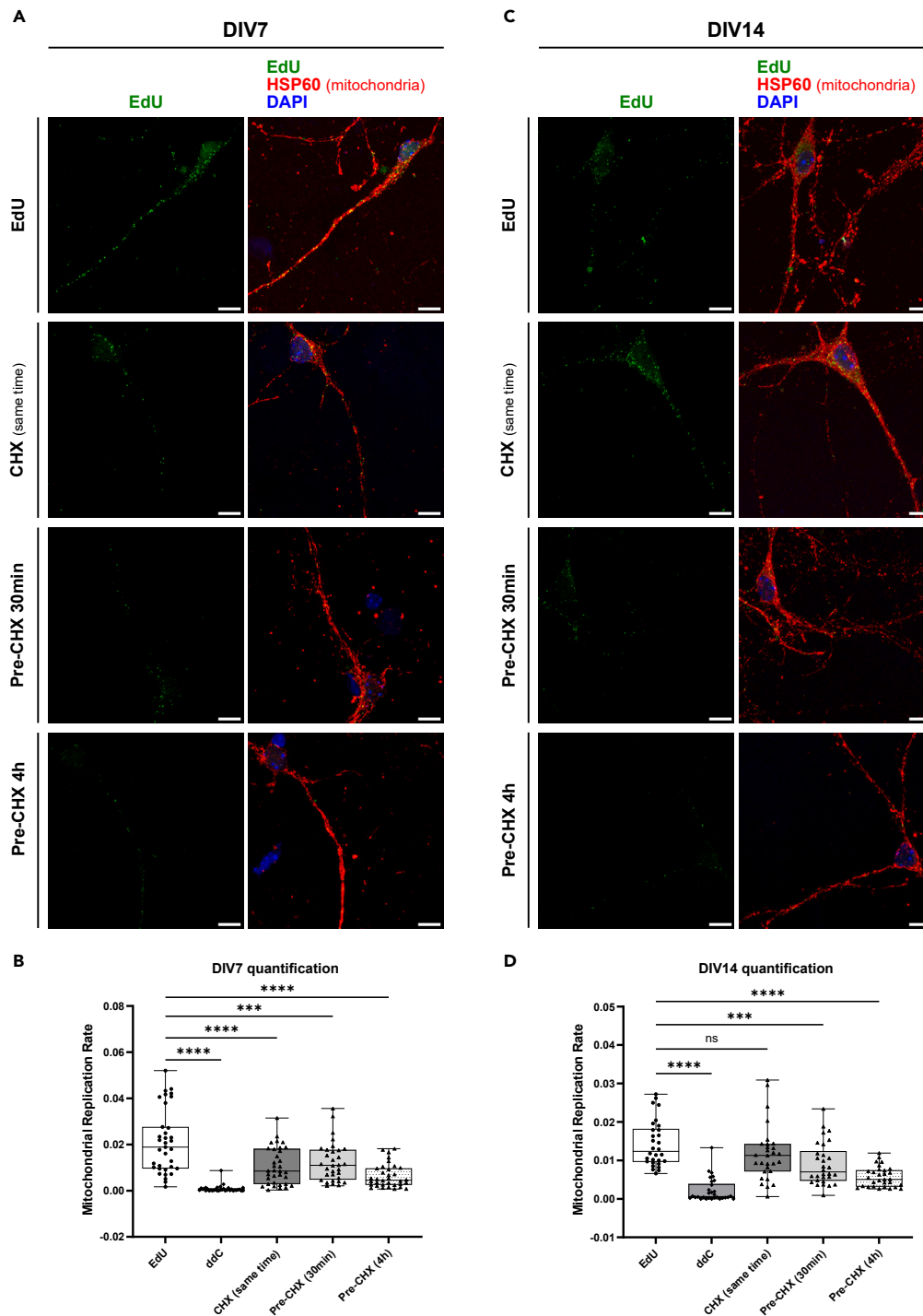
Figure 3. Mitochondrial replication in neurons requires *de novo* nuclear-encoded protein translation

(A and C) Representative images of mouse primary neurons at DIV7 (A) or at DIV14 (C) stained for EdU, in green, and for HSP60 (mitochondrial marker), in red. Neurons were incubated with EdU alone; Cycloheximide (CHX) at the same time as EdU; and pre-incubation of CHX for 30min or 4h, prior to EdU. Scale bar 10μm.

(B) Quantification of mitochondrial replication rate at DIV7. n = 32–35 neurons, from 3 independent experiments.

(D) Quantification of mitochondrial replication rate at DIV14. n = 29–30 neurons, from 3 independent experiments. One-way ANOVA with a Dunnet multiple comparison test (EdU as control). ns = non-significant; ***p < 0.001; ****p < 0.0001. Related to Figure S3.
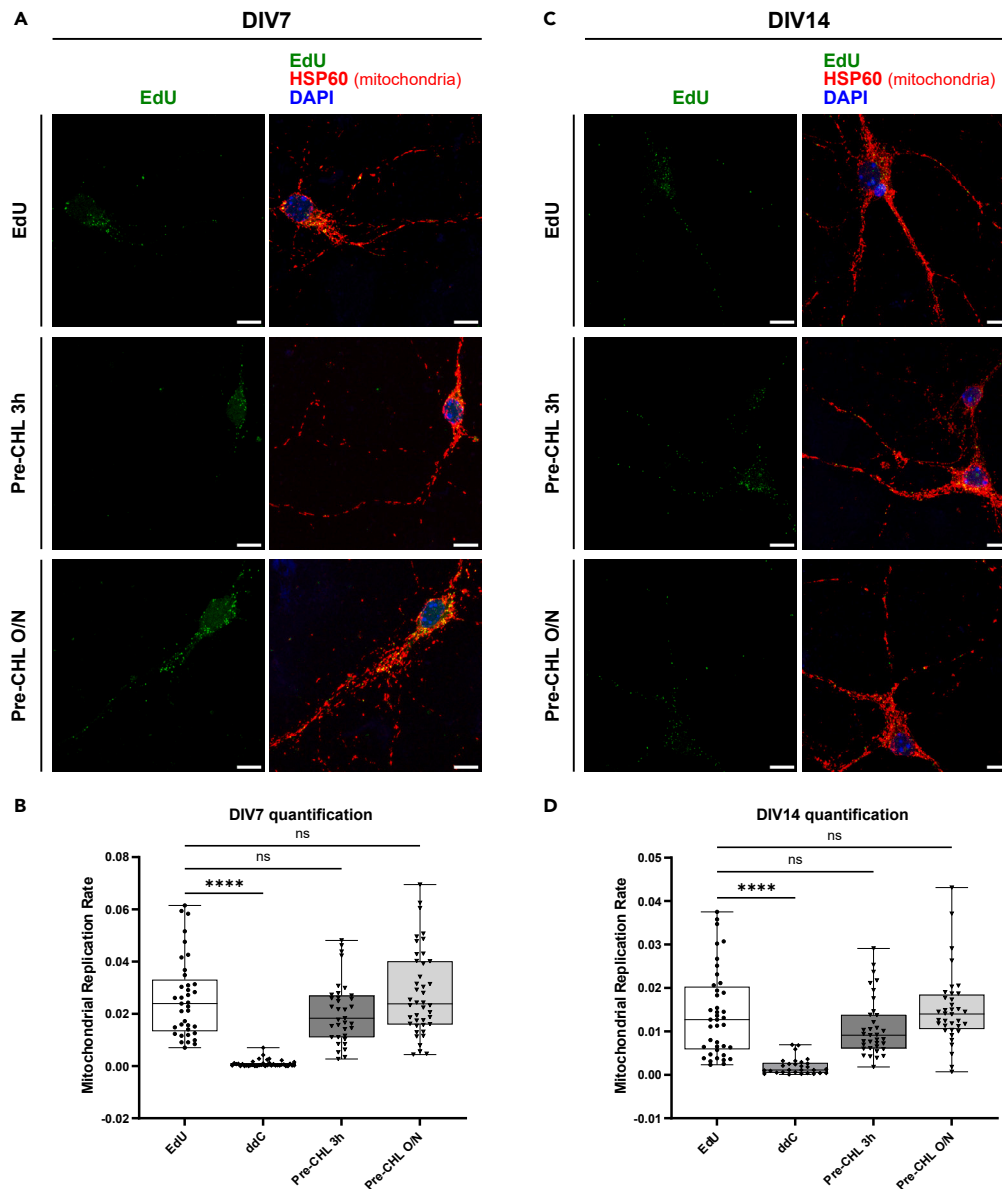
Figure 4. Mitochondrial-encoded protein translation is not required for mitochondrial replication in neurons

(A and C) Representative images of mouse primary neurons at DIV7 (A) or at DIV14 (C) stained for EdU, in green, and for HSP60 (mitochondrial marker), in red. Neurons were incubated with EdU alone; and pre-incubation of Chloramphenicol (CHL) for 3h or overnight (O/N), prior to EdU. Scale bar 10μm.

(B) Quantification of mitochondrial replication rate at DIV7. n = 35–42 neurons, from 3 independent experiments.

(D) Quantification of mitochondrial replication rate at DIV14. n = 29–40 neurons, from 3 independent experiments. One-way ANOVA with a Dunnet multiple comparison test (EdU as control). ns = non-significant; ****$p < 0.0001$. Related to Figure S4.

There was another elongation factor found upregulated in synaptic mitochondria, the mitochondrial elongation factor Tu (TUFM) (Figure 5E). Elongation factors are responsible for recruiting aminoacyl tRNAs to ribosomes, thus promoting protein translation. While eEF1A1 acts in the cytosol and is involved in nuclear-encoded protein translation, TUFM enters the mitochondria and is involved in mitochondrial-encoded protein translation. We hypothesize that these two elongation factors are responsible for promoting protein translation in the periphery of neurons, providing all the machinery necessary for mitochondria to replicate locally. In order to validate the proteomic results, we also assessed the levels of eEF1A1 and TUFM in synaptic and non-synaptic mitochondria through immunoblot analysis. As in the proteomic screen, eEF1A1 was more expressed in synaptic mitochondria when compared to non-synaptic mitochondria (Figure 5D). In the case of TUFM, we observed similar levels between the two fractions (Figure 5F). Although we could not validate the proteomic results through immunoblot, the fact that TUFM is present in synaptic mitochondria suggests that it may play a role in mitochondrial replication in the periphery of neurons.
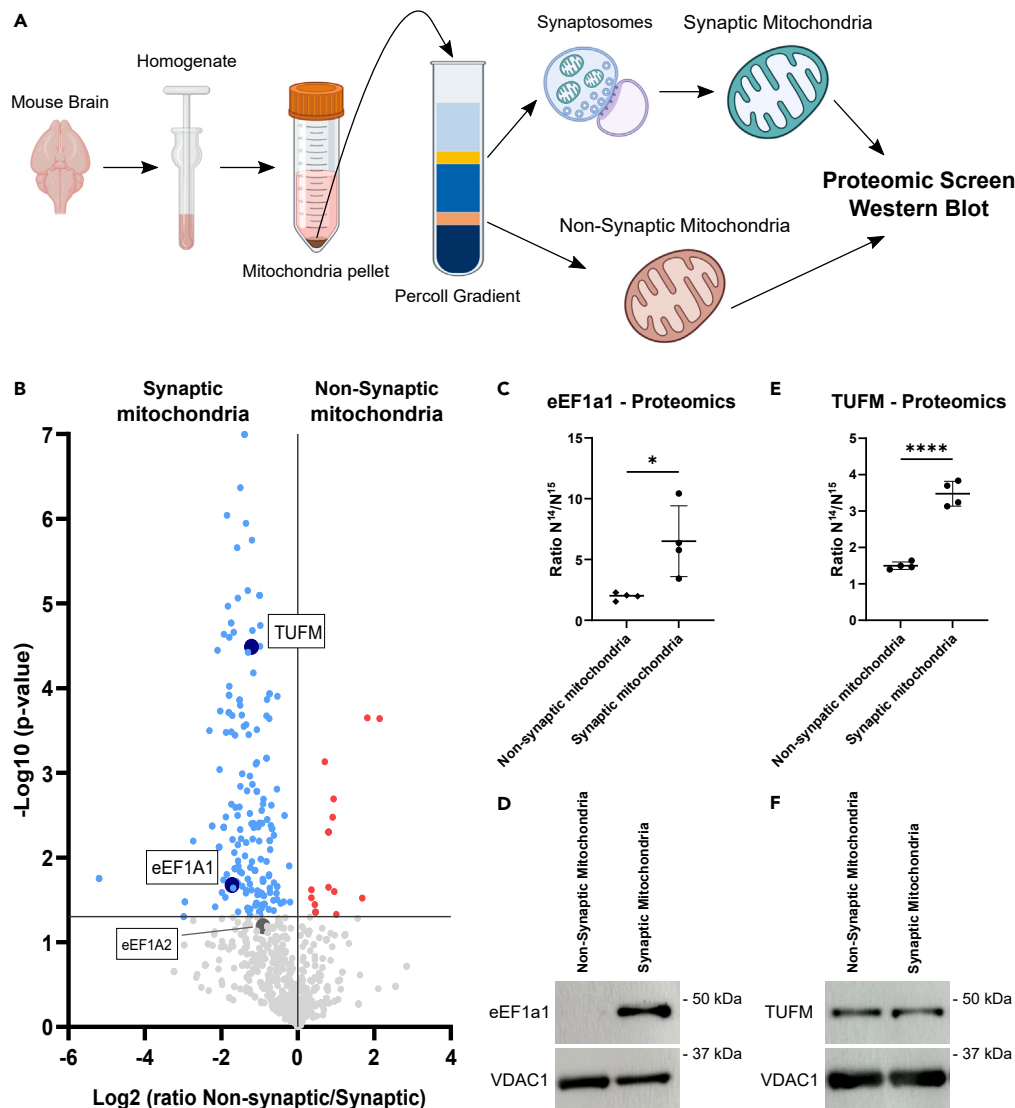
Figure 5. eEF1A1 and TUFM are upregulated in synaptic mitochondria

(A) Representative scheme of the isolation of synaptic and non-synaptic mitochondria from the mouse brain and the respective experimental design for the proteomic screen and immunoblot analysis.

(B) Volcano plot showing the relative levels of identified proteins in synaptic compared to non-synaptic mitochondria. The horizontal line defines the p value statistical significance cutoff ($p < 0.05$). Proteins with differences below the p value cut-off are depicted in gray. eEF1A2 is depicted in dark gray. Proteins with increased expression in non-synaptic mitochondria are depicted in red. Proteins with increased expression in synaptic mitochondria are depicted in light blue. eEF1A1 and TUFM are depicted in dark blue.

(C and E) Proteomic results of the relative levels comparing synaptic and non-synaptic mitochondria of eEF1A1 (C) and TUFM (E). Data represented as Mean ± SD. n = 4. Unpaired t-test. *$p < 0.05$; ****$p < 0.0001$ (D and F) Representative immunoblot images comparing synaptic and non-synaptic mitochondria for eEF1A1 (D) and TUFM (F) VDAC1 was used as a loading control.

TUFM is not involved in mitochondrial replication in mouse primary neurons

In the proteomic screen, we observed that TUFM is upregulated in synaptic mitochondria, which led us to speculate that it may be involved in mitochondrial replication in the periphery of neurons. To answer this question, we assessed the impact of TUFM downregulation on mitochondrial replication in neurons. We used a CFP-tagged shRNA against TUFM or a non-target RFP-tagged shRNA, as a control. As a rescue experiment, we co-transfected with an FLAG-tagged shRNA-resistant form of TUFM, or with a control plasmid coding for a V5-tagged mitochondrial targeting sequence. We validated these plasmids in N2a cells, a mouse neuroblastoma cell line. (Figures S6A and S6B). Mouse primary neurons were transfected 48h prior to incubation with EdU (Figures 6A–6C). Since in our hypothesis, the effect of TUFM would be specific to the periphery of neurons, we separated the somal from the periphery analysis. Neurons downregulated for TUFM presented similar levels
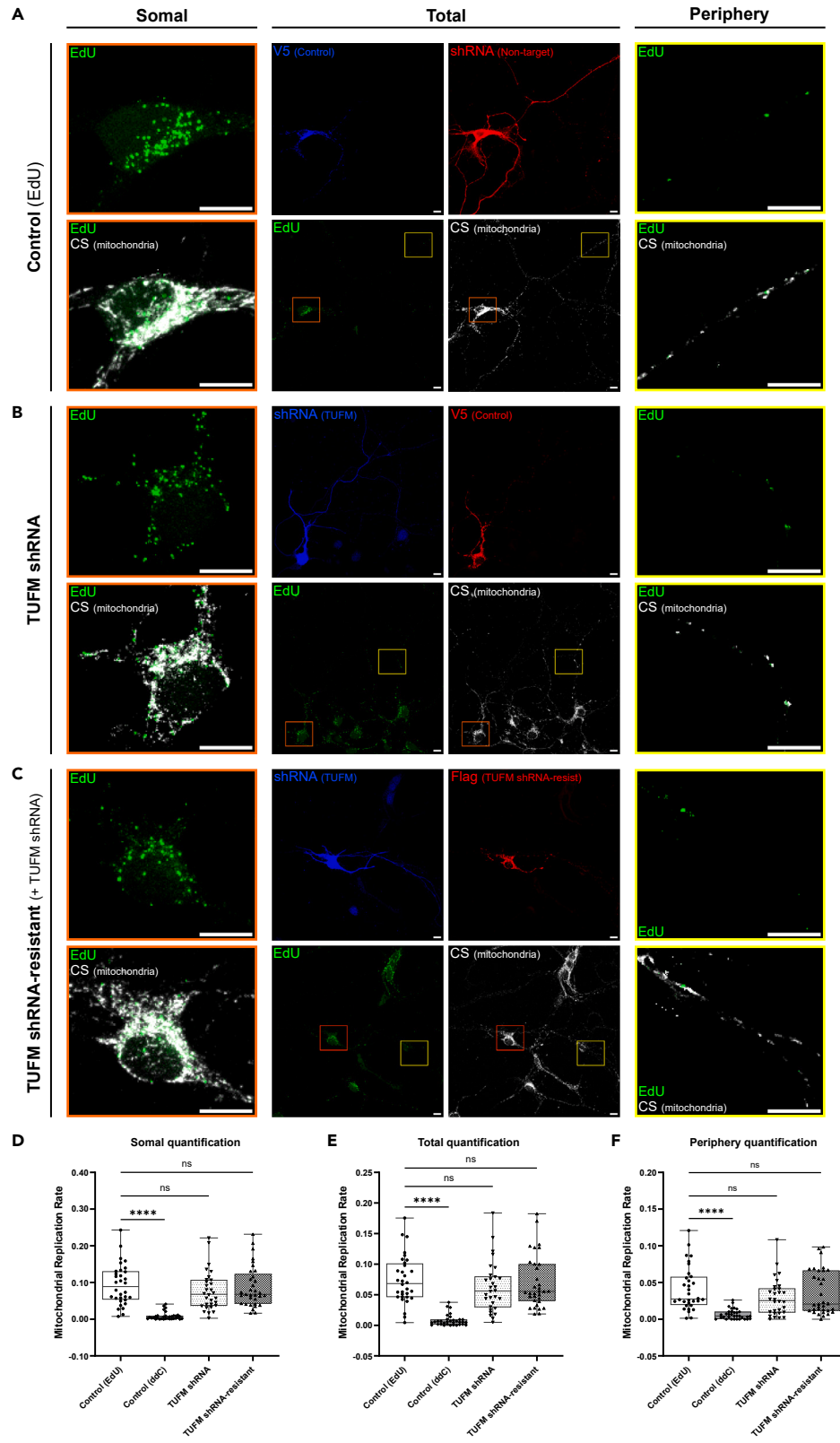
Figure 6. TUFM has no impact in mitochondrial replication in neurons

(A–C) Representative images of mouse primary neurons transfected with non-target RFP-tagged shRNA and V5-tagged mitochondrial targeting sequence (Control) (A); CFP-tagged TUFM shRNA and V5-tagged mitochondrial targeting sequence (TUFM downregulation) (B); or CFP-tagged TUFM shRNA and FLAG-tagged shRNA-resistant form of TUFM (rescue) (C). Neurons were also stained for EdU, in green, and for citrate synthase (mitochondrial marker), in white. Zoom in of the somal compartment in orange and zoom in on the periphery of neurons in yellow. Scale bar 10μm.

(D–F) Quantification of the mitochondrial replication rate in the soma (D); in the entire neuron (E) and in the periphery (F). For a particular transfected neuron, we defined a ROI for the somal part and the data outside that somal ROI was considered as periphery. Total quantification resulted from the sum of the somal and periphery quantifications. n = 30–33 neurons, from 4 independent experiments. One-way ANOVA with a Dunnet multiple comparison test (Control (EdU) as control). ns = non-significant; ****$p < 0.0001$. Experiments in Figures 6 and 7 were performed in parallel. The same controls were used. Related to Figure S6.

of EdU (Figures S6D, S6G, and S6J) and EdU co-localizing with mitochondria (Figures S6F, S6I, and S6L) when compared to control conditions. No significant differences in mitochondrial replication rate were observed in any of the conditions tested, neither at the soma nor at the periphery (Figures 6D–6F). In accordance with our results when neurons were incubated with chloramphenicol (Figure 4), *de novo* mitochondrial-encoded protein translation and TUFM are not required for mitochondrial replication to take place in neurons.

Eukaryotic translation elongation factor 1 alpha 1 is required for mitochondrial replication, particularly at the periphery of mouse primary neurons

Having established that mitochondrial replication in neurons requires *de novo* nuclear-encoded protein translation and that eEF1A1 is upregulated at the synapse, we hypothesized that eEF1A1 was promoting protein translation at the periphery of neurons, giving all the machinery necessary for mitochondria to replicate locally. Similar to the TUFM approach, we used an RFP-tagged shRNA against eEF1A1 or a non-target RFP-tagged shRNA, as a control. As a rescue experiment, we co-transfected with a V5-tagged shRNA-resistant form of eEF1A1, or with a control plasmid coding for a V5-tagged mitochondrial targeting sequence. We validated these plasmids in N2a cells. (Figures S7A and S7B). Mouse primary neurons were transfected for 48h and then were incubated with EdU (Figures 7A–7C). Since, in our hypothesis, the effect of eEF1A1 would be specific to the periphery of neurons, we performed the same sub-compartmentalized analysis mentioned above. When eEF1A1 was downregulated, we observed lower levels of EdU (Figure S7I) and EdU co-localizing with mitochondria (Figure S7K) specifically in the periphery of neurons. Regarding the mitochondrial replication rate, the downregulation of eEF1A1 led to a significantly decrease in all neuronal sub-compartments (Figures 7D–7F). However, this decrease was more pronounced in the periphery (Figure 7F). Moreover, overexpressing an shRNA-resistant form of eEF1A1 rescued the decreased levels of EdU (Figure S7I) and EdU co-localizing with mitochondria (Figure S7K) observed in the periphery of neurons downregulated for eEF1A1. Re-introducing eEF1A1 also rescued the mitochondrial replication rate to similar levels as observed in control conditions, both in the somal and in the periphery (Figures 7D–7F). Together these results indicate that although eEF1A1 may play a role in the soma, it is particularly important to maintain a healthy mitochondrial renewal at the periphery of neurons.

DISCUSSION

Our results reveal that mitochondria can replicate locally in the periphery of neurons. To achieve this, mitochondria require *de novo* nuclear-encoded protein translation, in a process involving the elongation factor eEF1A1.

Previous reports have validated that BrdU- and EdU-labelling can be used to observe mtDNA replication in neurons.[23,24,39] Our data also corroborate these findings. We then focused on developing an image analysis workflow to determine the mitochondrial replication rate. Although we were able to determine the mitochondrial replication rate using BrdU, the DNA denaturation step required in this protocol leads to alterations in the mitochondrial morphology. These alterations can cause artifacts when quantifying the mitochondrial staining. One can avoid this issue by using EdU instead of BrdU.

EdU-labelling also allows to localize where, within the cell, mitochondria replication may occur. This is particularly important in the context of neurons, where it has been shown that mitochondria in the soma differ from mitochondria in dendrites and axons.[1–3] It is generally assumed that mitochondria only replicate in the cell body and then travel to distal regions, such as synapses.[18–20] However, considering the neuronal length and the reduced mitochondrial transport observed in neurons,[21] mitochondrial replication must also take place distally. Using microfluidic devices, we confirmed that mitochondria can replicate locally in the periphery of neurons. This is in line with previous reports where mitochondrial replication has been shown to occur in axons.[23,24] Even though mitochondria are able to replicate in distal neuronal regions, we observed that most mitochondrial replication takes place in the cell body. Hence, this could suggest that mitochondrial turnover in the periphery of neurons is achieved not only by local replication, but also by mitochondria that replicated in the cell body and then travel to the neuron's periphery.

In the cell body and proximal neurites, renewal of mitochondria requires the activation of nuclear transcription, mediated by PGC-1α and NRF-1/2. In distal neuronal regions, away from the nucleus, it is unreasonable to think the same mechanism would also apply. Therefore, we postulate that, in the absence of new transcription, mitochondrial replication in the periphery of neurons is achieved by local translation. Mitochondria are composed of more than 1000 proteins, from which 13 are mitochondrial-encoded and the rest are nuclear-encoded proteins.[6] It has been reported that mRNAs coding for mitochondrial proteins are present in distal axons.[25,26] Additionally, the local translation of both mitochondrial-encoded[28] and nuclear-encoded[29,40,41] proteins occurs in axons. Our results show that mitochondrial replication is impaired when nuclear-encoded protein translation is inhibited with cycloheximide. Also, it has been previously reported that blocking axonal protein
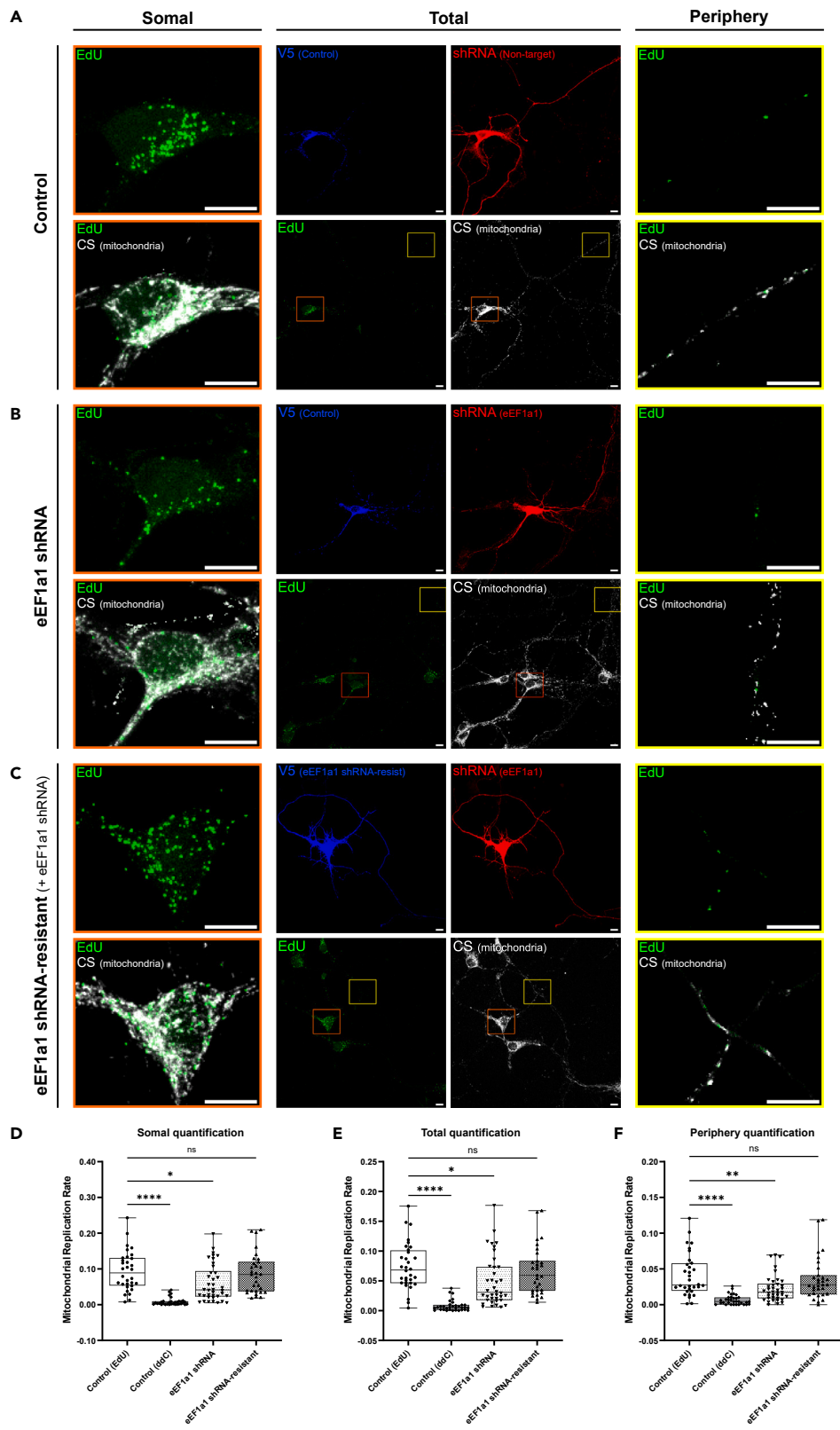
Figure 7. eEF1A1 is essential for mitochondrial replication in neurons, particularly at the periphery

(A–C) Representative images of mouse primary neurons transfected with non-target RFP-tagged shRNA and V5-tagged mitochondrial targeting sequence (Control) (A); RFP-tagged eEF1A1 shRNA and V5-tagged mitochondrial targeting sequence (eEF1A1 downregulation) (B); or RFP-tagged eEF1A1 shRNA and V5-tagged shRNA-resistant form of eEF1A1 (rescue) (C). Neurons were also stained for EdU, in green, and for Citrate Synthase (mitochondrial marker), in white. Zoom in on the somal compartment in orange and zoom in on the periphery of neurons in yellow. Scale bar 10μm.

(D–F) Quantification of the mitochondrial replication rate in the soma (D); in the entire neuron (E) and in the periphery (F). For a particular transfected neuron, we defined a ROI for the somal part and the data outside that somal ROI was considered as periphery. Total quantification resulted from the sum of the somal and periphery quantifications. n = 31–38 neurons, from 4 independent experiments. One-way ANOVA with a Dunnet multiple comparison test (Control (EdU) as control). ns = non-significant; *p < 0.05; **p < 0.01; ****p < 0.0001. Experiments in Figures 6 and 7 were performed in parallel. The same controls were used. Related to Figure S7.

translation leads to a decrease in mitochondrial membrane potential.[29,42] Together, these results suggest that the inability to keep a healthy mitochondrial turnover in the periphery of neurons, results in the accumulation of damaged mitochondria. Conversely, no differences were observed in mitochondrial replication when neurons were treated with chloramphenicol, an inhibitor of mitochondrial-encoded protein translation. This can be explained by the observation that the 13 proteins encoded in the mtDNA are all part of the OXPHOS system, and all the proteins involved in mitochondrial replication are nuclear-encoded.

To decipher the mechanisms linking protein synthesis and mitochondrial replication, we performed a proteomic screen comparing synaptic and non-synaptic mitochondria. We found two elongation factors –TUFM and eEF1A1– upregulated in the synaptic pool. While TUFM enters the mitochondria and is involved in mitochondrial-encoded protein translation, eEF1A1 acts in the cytosol and promotes nuclear-encoded protein translation. The observation of eEF1A1 (a cytosolic protein) in isolated mitochondria may seem unexpected; however, as nuclear-encoded mitochondrial proteins are being translated, they are being directed to mitochondria. This way placing the translation machinery in the vicinity of mitochondria.

In accordance with the results observed upon the inhibition of mitochondrial-encoded protein translation (chloramphenicol treatment), downregulation of TUFM had no impact on mitochondrial replication in neurons, neither in the soma nor in the periphery. This suggests that mitochondrial replication in neurons does not require the *de novo* translation of mitochondrial-encoded proteins. Nonetheless, as mitochondrial-encoded protein translation is essential to maintain the membrane potential of axonal mitochondria,[42] TUFM may be important to keep a proper mitochondrial function at synapse. Interestingly, in this study, we show that the mitochondrial replication rate is impaired when eEF1A1 is downregulated and that this impairment is more pronounced in the periphery of neurons. It has been postulated that during neurodevelopment, eEF1A1 is replaced by its homologue eEF1A2.[35,36] Here we corroborate previous data, where rather than a complete change in the expression of eEF1A1 to eEF1A2, there is a change in the localization of eEF1A1 from the soma to the periphery of neurons.[37,38,43] This implies that the decreased mitochondrial replication observed in the soma upon the downregulation of eEF1A1, may only be observed in embryonic primary neurons, and may not be relevant in the context of adult neurons. On the other hand, mitochondrial replication in the periphery of neurons relies almost exclusively on eEF1A1.

Mitochondria play a crucial role in supplying neurons with ATP. This is particularly important during stimulation, where blocking mitochondrial-driven ATP synthesis leads to synaptic dysfunction.[44,45] One of the many processes that requires high levels of ATP consumption at the synapse is local protein translation. Each peptide bond formed consumes 4 molecules of ATP[46] and it is estimated that synaptic proteins are turned over at the order of more than 1000 copies per minute.[47] This rapid protein turnover is essential for synaptic plasticity and is fueled by mitochondria.[44] On the other hand, our data indicate that protein synthesis is required for mitochondrial replication in the periphery of neurons. It has also been reported that synaptic stimulation leads to an increase in mitochondrial replication.[48] These results suggest the existence of a positive feedback loop, where, during synaptic stimulation, mitochondria fuel local protein synthesis, leading to the formation of new mitochondria, essential to support neuronal plasticity. Here, we have shown that eEF1A1 is crucial for mitochondrial replication in the distal region of neurons. However, at present, the eEF1A1 counterparts and the regulatory mechanisms of such molecular signaling pathways remain unknown.

Our study unravels the mechanisms that lead to mitochondrial replication in distal regions of neurons. This is particularly important in the context of neurodegeneration, where synaptic defects are observed prior to neuronal loss. Understanding how mitochondria replicate at the synapse will give us new insights into the pathophysiology at the early stages of neurodegenerative diseases and may ultimately lead to the development of new therapies to prevent the progression of these disorders.

Limitations of the study

In this study, we could only address the role of TUFM and eEF1A1 on mitochondrial replication, in the periphery of neurons, which includes dendrites and axons. Although, in Figure 2 we demonstrate that mitochondrial replication occurs specifically in axons; in the experimental setup of Figures 6 and 7, it is technically unfeasible to discriminate between the two neuronal regions.

STAR★METHODS

Detailed methods are provided in the online version of this paper and include the following:

- KEY RESOURCES TABLE

SUPPLEMENTAL INFORMATION

Supplemental information can be found online at https://doi.org/10.1016/j.isci.2024.109136.

AUTHOR CONTRIBUTIONS

CCR and RAS performed and analyzed the chloramphenicol experiments. MS, with technical support from KC and VAM, developed the brain mitochondrial sub fractionation protocol. YZW; AFP; EBW; and JNS performed and analyzed the N^{15} proteomic screen. CCR performed and analyzed the remaining experiments. CCR and VAM designed the research and wrote the article. All authors have read and agreed to the published version of the article.

DECLARATION OF INTERESTS

All authors have nothing to declare.

REFERENCES

1. Kiebish, M.A., Han, X., Cheng, H., Lunceford, A., Clarke, C.F., Moon, H., Chuang, J.H., Seyfried, T.N., Luncedord, A., Clarke, C.F., et al. (2008). Lipidomic analysis and electron transport chain activities in C57BL/6J mouse brain mitochondria. J. Neurochem. *106*, 299–312. https://doi.org/10.1111/j.1471-4159.2008.05383.x.

2. Stauch, K.L., Purnell, P.R., and Fox, H.S. (2014). Quantitative proteomics of synaptic and nonsynaptic mitochondria: Insights for synaptic mitochondrial vulnerability. J. Proteome Res. *13*, 2620–2636. https://doi.org/10.1021/pr500295n.

3. Völgyi, K., Gulyássy, P., Háden, K., Kis, V., Badics, K., Kékesi, K.A., Simor, A., Györffy, B., Tóth, E.A., Lubec, G., et al. (2015). Synaptic mitochondria: A brain mitochondria cluster with a specific proteome. J. Proteomics *120*, 142–157. https://doi.org/10.1016/j.jprot.2015.03.005.

4. Chen, H., and Chan, D.C. (2009). Mitochondrial dynamics-fusion, fission, movement, and mitophagy-in neurodegenerative diseases. Hum. Mol. Genet. *18*, R169–R176. https://doi.org/10.1093/hmg/ddp326.

5. Flippo, K.H., and Strack, S. (2017). Mitochondrial dynamics in neuronal injury, development and plasticity. J. Cell Sci. *130*, 671–681. https://doi.org/10.1242/JCS.171017.

6. Rath, S., Sharma, R., Gupta, R., Ast, T., Chan, C., Durham, T.J., Goodman, R.P., Grabarek, Z., Haas, M.E., Hung, W.H.W., et al. (2021). MitoCarta3.0: an updated mitochondrial proteome now with sub-organelle localization and pathway annotations. Nucleic Acids Res. *49*, D1541–D1547. https://doi.org/10.1093/nar/gkaa1011.

7. Cardanho-Ramos, C., and Morais, V.A. (2021). Mitochondrial Biogenesis in Neurons: How and Where. Int. J. Mol. Sci. *22*, 13059. https://doi.org/10.3390/IJMS222313059.

8. Diaz, F., and Moraes, C.T. (2008). Mitochondrial biogenesis and turnover. Cell Calcium *44*, 24–35. https://doi.org/10.1016/j.ceca.2007.12.004.

9. Jornayvaz, F.R., and Shulman, G.I. (2010). Regulation of mitochondrial biogenesis. Essays Biochem. *47*, 69–84. https://doi.org/10.1042/BSE0470069.

10. Ma, D., Li, S., Lucas, E.K., Cowell, R.M., and Lin, J.D. (2010). Neuronal inactivation of peroxisome proliferator-activated receptor γ coactivator 1α (PGC-1α) protects mice from diet-induced obesity and leads to degenerative lesions. J. Biol. Chem. *285*, 39087–39095. https://doi.org/10.1074/JBC.M110.151688.

11. Cui, L., Jeong, H., Borovecki, F., Parkhurst, C.N., Tanese, N., and Krainc, D. (2006). Transcriptional repression of PGC-1alpha by mutant huntingtin leads to mitochondrial dysfunction and neurodegeneration. Cell *127*, 59–69. https://doi.org/10.1016/J.CELL.2006.09.015.

12. Stevens, D.A., Lee, Y., Kang, H.C., Lee, B.D., Lee, Y.I., Bower, A., Jiang, H., Kang, S.U., Andrabi, S.A., Dawson, V.L., et al. (2015). Parkin loss leads to Paris-dependent declines in mitochondrial mass and respiration. Proc. Natl. Acad. Sci. USA *112*, 11696–11701. https://doi.org/10.1073/PNAS.1500624112.

13. Shin, J.H., Ko, H.S., Kang, H., Lee, Y., Lee, Y.I., Pletinkova, O., Troconso, J.C., Dawson, V.L., and Dawson, T.M. (2011). PARIS (ZNF746) repression of PGC-1α contributes to neurodegeneration in parkinson's disease. Cell *144*, 689–702. https://doi.org/10.1016/J.CELL.2011.02.010.

14. Dölle, C., Flønes, I., Nido, G.S., Miletic, H., Osuagwu, N., Kristoffersen, S., Lilleng, P.K., Larsen, J.P., Tysnes, O.B., Haugarvoll, K., et al. (2016). Defective mitochondrial DNA homeostasis in the substantia nigra in Parkinson disease. Nat. Commun. *7*, 13548. https://doi.org/10.1038/ncomms13548.

15. Sheng, B., Wang, X., Su, B., Lee, H.G., Casadesus, G., Perry, G., and Zhu, X. (2012). Impaired mitochondrial biogenesis contributes to mitochondrial dysfunction in Alzheimer's disease. J. Neurochem. *120*, 419–429. https://doi.org/10.1111/J.1471-4159.2011.07581.X.

16. Zhu, X., Perry, G., Moreira, P.I., Aliev, G., Cash, A.D., Hirai, K., and Smith, M.A. (2006). Mitochondrial abnormalities and oxidative imbalance in Alzheimer disease. J. Alzheimers Dis. *9*, 147–153. https://doi.org/10.3233/JAD-2006-9207.

17. Ekstrand, M.I., Terzioglu, M., Galter, D., Zhu, S., Hofstetter, C., Lindqvist, E., Thams, S., Bergstrand, A., Hansson, F.S., Trifunovic, A., et al. (2007). Progressive parkinsonism in mice with respiratory-chain-deficient dopamine neurons. Proc. Natl. Acad. Sci. USA *104*, 1325–1330. https://doi.org/10.1073/pnas.0605208103.

18. Davis, A.F., and Clayton, D.A. (1996). In situ localization of mitochondrial DNA replication in intact mammalian cells. J. Cell Biol. *135*, 883–893. https://doi.org/10.1083/JCB.135.4.883.

19. Fedorovich, S.V., Waseem, T.V., and Puchkova, L.V. (2017). Biogenetic and morphofunctional heterogeneity of mitochondria: The case of synaptic mitochondria. Rev. Neurosci. *28*, 363–373. https://doi.org/10.1515/revneuro-2016-0077.

20. Li, P.A., Hou, X., and Hao, S. (2017). Mitochondrial biogenesis in neurodegeneration. J. Neurosci. Res. *95*, 2025–2029. https://doi.org/10.1002/JNR.24042.

21. Misgeld, T., and Schwarz, T.L. (2017). Mitostasis in Neurons: Maintaining Mitochondria in an Extended Cellular Architecture. Neuron *96*, 651–666. https://doi.org/10.1016/J.NEURON.2017.09.055.

22. Price, J.C., Guan, S., Burlingame, A., Prusiner, S.B., and Ghaemmaghami, S. (2010). Analysis of proteome dynamics in the mouse brain. Proc. Natl. Acad. Sci. USA *107*, 14508–14513. https://doi.org/10.1073/PNAS.1006551107.

23. Amiri, M., and Hollenbeck, P.J. (2008). Mitochondrial biogenesis in the axons of vertebrate peripheral neurons. Dev. Neurobiol. *68*, 1348–1361. https://doi.org/10.1002/dneu.20668.

24. Van Laar, V.S., Arnold, B., Howlett, E.H., Calderon, M.J., St. Croix, C.M., Greenamyre, J.T., Sanders, L.H., and Berman, S.B. (2018). Evidence for Compartmentalized Axonal Mitochondrial Biogenesis: Mitochondrial DNA Replication Increases in Distal Axons As an Early Response to Parkinson's Disease-Relevant Stress. J. Neurosci. *38*, 7505–7515. https://doi.org/10.1523/JNEUROSCI.0541-18.2018.

25. Aschrafi, A., Kar, A.N., Gale, J.R., Elkahloun, A.G., Vargas, J.N.S., Sales, N., Wilson, G., Tompkins, M., Gioio, A.E., and Kaplan, B.B. (2016). A heterogeneous population of nuclear-encoded mitochondrial mRNAs is present in the axons of primary sympathetic neurons. Mitochondrion *30*, 18–23. https://doi.org/10.1016/J.MITO.2016.06.002.

26. Shigeoka, T., Jung, H., Jung, J., Turner-Bridger, B., Ohk, J., Lin, J.Q., Amieux, P.S., and Holt, C.E. (2016). Dynamic Axonal Translation in Developing and Mature Visual Circuits. Cell *166*, 181–192. https://doi.org/10.1016/J.CELL.2016.05.029.

27. Tushev, G., Glock, C., Heumüller, M., Biever, A., Jovanovic, M., and Schuman, E.M. (2018). Alternative 3′ UTRs Modify the Localization, Regulatory Potential, Stability, and Plasticity of mRNAs in Neuronal Compartments. Neuron *98*, 495–511.e6. https://doi.org/10.1016/J.NEURON.2018.03.030.

28. Yousefi, R., Fornasiero, E.F., Cyganek, L., Montoya, J., Jakobs, S., Rizzoli, S.O., Rehling, P., and Pacheu-Grau, D. (2021). Monitoring mitochondrial translation in living cells. EMBO Rep. *22*, e51635. https://doi.org/10.15252/EMBR.202051635.

29. Cioni, J.M., Lin, J.Q., Holtermann, A.V., Koppers, M., Jakobs, M.A.H., Azizi, A., Turner-Bridger, B., Shigeoka, T., Franze, K., Harris, W.A., and Holt, C.E. (2019). Late Endosomes Act as mRNA Translation Platforms and Sustain Mitochondria in Axons. Cell *176*, 56–72.e15. https://doi.org/10.1016/j.cell.2018.11.030.

30. Kuzniewska, B., Cysewski, D., Wasilewski, M., Sakowska, P., Milek, J., Kulinski, T.M., Winiarski, M., Kozielewicz, P., Knapska, E., Dadlez, M., et al. (2020). Mitochondrial protein biogenesis in the synapse is supported by local translation. EMBO Rep. *21*, e48882. https://doi.org/10.15252/EMBR.201948882.

31. Salic, A., and Mitchison, T.J. (2008). A chemical method for fast and sensitive detection of DNA synthesis *in vivo*. Proc. Natl. Acad. Sci. USA *105*, 2415–2420. https://doi.org/10.1073/PNAS.0712168105.

32. Taylor, A.M., Blurton-Jones, M., Rhee, S.W., Cribbs, D.H., Cotman, C.W., and Jeon, N.L. (2005). A microfluidic culture platform for CNS axonal injury, regeneration and transport. Nat. Methods *2*, 599–605. https://doi.org/10.1038/NMETH777.

33. Obrig, T.G., Culp, W.J., McKeehan, W.L., and Hardesty, B. (1971). The Mechanism by which Cycloheximide and Related Glutarimide Antibiotics Inhibit Peptide Synthesis on Reticulocyte Ribosomes. J. Biol. Chem. *246*, 174–181. https://doi.org/10.1016/S0021-9258(18)62546-3.

34. Faria-Pereira, A., Temido-Ferreira, M., and Morais, V.A. (2022). BrainPhys Neuronal Media Support Physiological Function of Mitochondria in Mouse Primary Neuronal Cultures. Front. Mol. Neurosci. *15*, 837448. https://doi.org/10.3389/FNMOL.2022.837448.

35. Pan, J., Ruest, L.B., Xu, S., and Wang, E. (2004). Immuno-characterization of the switch of peptide elongation factors eEF1A-1/EF-1alpha and eEF1A-2/S1 in the central nervous system during mouse development. Dev. Brain Res. *149*, 1–8. https://doi.org/10.1016/J.DEVBRAINRES.2003.10.011.

36. Khalyfa, A., Bourbeau, D., Chen, E., Petroulakis, E., Pan, J., Xu, S., and Wang, E. (2001). Characterization of elongation factor-1A (eEF1A-1) and eEF1A-2/S1 protein expression in normal and wasted mice.

J. Biol. Chem. *276*, 22915–22922. https://doi.org/10.1074/JBC.M101011200.

37. Glock, C., Biever, A., Tushev, G., Nassim-Assir, B., Kao, A., Bartnik, I., Tom Dieck, S., and Schuman, E.M. (2021). The translatome of neuronal cell bodies, dendrites, and axons. Proc. Natl. Acad. Sci. USA *118*, e2113929118. https://doi.org/10.1073/PNAS.2113929118.

38. Davies, F.C.J., Marshall, G.F., Pegram, E., Gadd, D., and Abbott, C.M. (2023). Endogenous epitope tagging of eEF1A2 in mice reveals early embryonic expression of eEF1A2 and subcellular compartmentalisation of neuronal eEF1A1 and eEF1A2. Mol. Cell. Neurosci. *126*, 103879. https://doi.org/10.1016/j.mcn.2023.103879.

39. Lentz, S.I., Edwards, J.L., Backus, C., McLean, L.L., Haines, K.M., and Feldman, E.L. (2010). Mitochondrial DNA (mtDNA) biogenesis: Visualization and duel incorporation of BrdU and EdU into newly synthesized mtDNA *in vitro*. J. Histochem. Cytochem. *58*, 207–218. https://doi.org/10.1369/JHC.2009.954701.

40. Cosker, K.E., Fenstermacher, S.J., Pazyra-Murphy, M.F., Elliott, H.L., and Segal, R.A. (2016). The RNA-binding protein SFPQ orchestrates an RNA regulon to promote axon viability. Nat. Neurosci. *19*, 690–696. https://doi.org/10.1038/nn.4280.

41. Yoon, B.C., Jung, H., Dwivedy, A., O'Hare, C.M., Zivraj, K.H., and Holt, C.E. (2012). Local translation of extranuclear lamin B promotes axon maintenance. Cell *148*, 752–764. https://doi.org/10.1016/j.cell.2011.11.064.

42. Hillefors, M., Gioio, A.E., Mameza, M.G., and Kaplan, B.B. (2007). Axon viability and mitochondrial function are dependent on local protein synthesis in sympathetic neurons. Cell. Mol. Neurobiol. *27*, 701–716. https://doi.org/10.1007/S10571-007-9148-Y.

43. Wefers, Z., Alecki, C., Huang, R., Jacob-Tomas, S., and Vera, M. (2022). Analysis of the Expression and Subcellular Distribution of eEF1A1 and eEF1A2 mRNAs during Neurodevelopment. Cells *11*, 1877. https://doi.org/10.3390/CELLS11121877.

44. Rangaraju, V., Lauterbach, M., and Schuman, E.M. (2019). Spatially Stable Mitochondrial Compartments Fuel Local Translation during Plasticity. Cell *176*, 73–84.e15. https://doi.org/10.1016/j.cell.2018.12.013.

45. Rangaraju, V., Calloway, N., and Ryan, T.A. (2014). Activity-Driven Local ATP Synthesis Is Required for Synaptic Function. Cell *156*, 825–835. https://doi.org/10.1016/j.cell.2013.12.042.

46. Harris, J.J., and Attwell, D. (2012). The energetics of CNS white matter. J. Neurosci. *32*, 356–371. https://doi.org/10.1523/JNEUROSCI.3430-11.2012.

47. Cohen, L.D., Zuchman, R., Sorokina, O., Müller, A., Dieterich, D.C., Armstrong, J.D., Ziv, T., and Ziv, N.E. (2013). Metabolic Turnover of Synaptic Proteins: Kinetics, Interdependencies and Implications for Synaptic Maintenance. PLoS One *8*, e63191. https://doi.org/10.1371/JOURNAL.PONE.0063191.

48. Yu, L., and Yang, S.J. (2010). AMP-activated protein kinase mediates activity-dependent regulation of peroxisome proliferator-activated receptor gamma coactivator-1alpha and nuclear respiratory factor 1 expression in rat visual cortical neurons. Neuroscience *169*, 23–38. https://doi.org/10.1016/J.NEUROSCIENCE.2010.04.063.

49. Percie du Sert, N., Ahluwalia, A., Alam, S., Avey, M.T., Baker, M., Browne, W.J., Clark, A., Cuthill, I.C., Dirnagl, U., Emerson, M., et al. (2020). Reporting animal research: Explanation and elaboration for the ARRIVE guidelines 2.0. PLoS Biol. *18*, e3000411. https://doi.org/10.1371/JOURNAL.PBIO.3000411.

50. Harris, J., Lee, H., Tu, C.T., Cribbs, D., Cotman, C., and Jeon, N.L. (2007). Preparing e18 cortical rat neurons for compartmentalization in a microfluidic device. J. Vis. Exp. *8*, 305. https://doi.org/10.3791/305-V.

51. Sims, N.R., and Anderson, M.F. (2008). Isolation of mitochondria from rat brain using Percoll density gradient centrifugation. Nat. Protoc. *3*, 1228–1239. https://doi.org/10.1038/nprot.2008.105.

52. Savas, J.N., Toyama, B.H., Xu, T., Yates, J.R., and Hetzer, M.W. (2012). Extremely long-lived nuclear pore proteins in the rat brain. Science *335*, 942. https://doi.org/10.1126/science.1217421.

53. Savas, J.N., Park, S.K., and Yates, J.R. (2016). Proteomic analysis of protein turnover by metabolic whole rodent pulse-chase isotopic labeling and shotgun mass spectrometry analysis. Methods Mol. Biol. *1410*, 293–304. https://doi.org/10.1007/978-1-4939-3524-6_18.

54. Wiśniewski, J.R., Zougman, A., Nagaraj, N., and Mann, M. (2009). Universal sample preparation method for proteome analysis. Nat. Methods *6*, 359–362. https://doi.org/10.1038/nmeth.1322.

55. Savas, J.N., Ribeiro, L.F., Wierda, K.D., Wright, R., DeNardo-Wilke, L.A., Rice, H.C., Chamma, I., Wang, Y.-Z., Zemla, R., Lavallée-Adam, M., et al. (2015). The Sorting Receptor SorCS1 Regulates Trafficking of Neurexin and AMPA Receptors. Neuron *87*, 764–780. https://doi.org/10.1016/j.neuron.2015.08.007.

56. Eng, J.K., McCormack, A.L., and Yates, J.R. (1994). An approach to correlate tandem mass spectral data of peptides with amino acid sequences in a protein database. J. Am. Soc. Mass Spectrom. *5*, 976–989. https://doi.org/10.1016/1044-0305(94)80016-2.

57. Xu, T., Park, S.K., Venable, J.D., Wohlschlegel, J.A., Diedrich, J.K., Cociorva, D., Lu, B., Liao, L., Hewel, J., Han, X., et al. (2015). ProLuCID: An improved SEQUEST-like algorithm with enhanced sensitivity and specificity. J. Proteomics *129*, 16–24. https://doi.org/10.1016/j.jprot.2015.07.001.

58. Cociorva, D., L Tabb, D., and Yates, J.R. (2007). Validation of tandem mass spectrometry database search results using DTASelect. Curr. Protoc. Bioinforma. *Chapter 13*. Unit 13.4. https://doi.org/10.1002/0471250953.bi1304s16.

59. Tabb, D.L., McDonald, W.H., and Yates, J.R. (2002). DTASelect and contrast: Tools for assembling and comparing protein identifications from shotgun proteomics. J. Proteome Res. *1*, 21–26. https://doi.org/10.1021/pr015504q.

60. UniProt Consortium (2015). UniProt: a hub for protein information. Nucleic Acids Res. *43*, D204–D212. https://doi.org/10.1093/nar/gku989.

STAR★METHODS

KEY RESOURCES TABLE

REAGENT or RESOURCE	SOURCE	IDENTIFIER
Antibodies		
Anti-BrdU	Bio-Rad	MCA2483GA
Anti-Citrate Synthase	Proteintech	16131-1-AP; RRID: AB_1640013
Anti-HSP60	BD Biosciences	611563; RRID: AB_399009
Anti-β3 tubulin	BioLegend	802001; RRID: AB_2564645
Anti-MAP2	Sigma-Aldrich	MAB3418; RRID: AB_94856
Anti-Puromycin	Kerafast	EQ0001; RRID: AB_2620162
Anti-VDAC1	Abcam	ab154856; RRID: AB_2687466
Anti-TUFM	Abcam	ab173300; RRID: AB_2750903
Anti-eEF1A1	Abcam	ab157455
Anti-V5	Invitrogen	R960-25; RRID: AB_2556564
Anti-Flag	Sigma-Aldrich	F3165; RRID: AB_259529
Anti-tagRFP	Cancer Tools (BrainBow)	155265
Anti-GFP (CFP)	Abcam	ab13970; RRID: AB_300798
Anti-GAPDH	Invitrogen	AM4300; RRID: AB_2536381
Anti-GFAP	Sigma-Aldrich	G9269; RRID: AB_477035
Anti-PSD95	Enzo Life Sciences	ADI-VAM-PS002-E; RRID: AB_11180787
Anti-Synaptophysin 1	Synaptic Systems	101011; RRID: AB_887824
Alexa Fluor 488 Azide	Jena BioScience	CLK-1275
Alexa Fluor 568 Anti-Mouse	Invitrogen	A11031; RRID: AB_144696
Alexa Fluor 568 Anti-Chicken	Invitrogen	A78950; RRID: AB_2921072
Alexa Fluor 405 Anti-Mouse	Invitrogen	A48255; RRID: AB_2890536
Alexa Fluor 405 Anti-Chicken	Invitrogen	A48260; RRID: AB_2890271
Alexa Fluor 488 Anti-Rabbit	Invitrogen	A21206; RRID: AB_2535792
Alexa Fluor 647 Anti-Rabbit	Invitrogen	A31573; RRID: AB_2536183
HRP Conjugated Anti-Mouse	Bio-Rad	1706516; RRID: AB_2921252
HRP Conjugated Anti-Rabbit	Bio-Rad	1706515; RRID: AB_11125142
Chemicals, peptides, and recombinant proteins		
5-Bromo-2'-deoxyuridine (BrdU)	Sigma-Aldrich	B5002
2'-Deoxy-5-ethynyluridine (EdU)	Carbosynth	NE08701
DAPI	Sigma-Aldrich	D9542
2',3'-DiDeoxyCitidine (ddC)	Sigma-Aldrich	D5782
Puromycin	Sigma-Aldrich	P8833
L-Homopropargylglycine (HPG)	Invitrogen	C10186
Cycloheximide (CHX)	Abcam	ab120093
Chloramphenicol (CHL)	Sigma-Aldrich	C1919
Paraformaldehyde (PFA)	Electron Microscopy Sciences	15710
Bovine Serum Albumin (BSA)	Sigma-Aldrich	A9647
Copper(II) sulfate pentahydrate ($CuSO_4.5H_2O$)	Sigma-Aldrich	209198
Ascorbic Acid	Sigma-Aldrich	255564
Kynurenic Acid	Sigma-Aldrich	K3375
Lipofectamine 2000	Invitrogen	11668027

Continued

REAGENT or RESOURCE	SOURCE	IDENTIFIER
Dulbecco's Modified Eagle Medium/ Nutrient Mixture F-12 (DMEM-F12)	Gibco	11039047
Fetal Bovine Serum (FBS)	Gibco	A3840402
Hank's Balanced Salt Solution (HBSS)	Gibco	14175095
HEPES	Gibco	15630056
Trypsin	Gibco	15090046
DNase I	Sigma-Aldrich	DN25
Horse Serum (HS)	Gibco	2605088
Minimum Essential Medium (MEM)	Gibco	31095029
Glucose	Gibco	A2494001
Penicillin-Streptomycin	Gibco	15140122
Poly D-Lysine	Sigma-Aldrich	P7280
NeuroBasal medium (NB)	Gibco	21103049
L-Glutamine	ThermoScientific	25030024
B-27	Gibco	17504044
VectaShield® Antifade Mounting Medium	Vector laboratories	H-1000
Sucrose	Sigma-Aldrich	84100
D-Mannitol	Sigma-Aldrich	M4125
EGTA	Sigma-Aldrich	E4378
Percoll	Sigma-Aldrich	GE17-0891-02
Digitonin	Sigma-Aldrich	D141
Protease Inhibitor	ThermoScientific	78443
Urea	ThermoScientific	29700
Ammonium bicarbonate solution	Fluka	09830
ProteaseMAX	Promega	V2072
Tris(2-carboxyethyl)phosphine (TCEP)	Sigma-Aldrich	C4706
Iodoacetamide (IAA)	Sigma-Aldrich	1149
Trypsin	Promega	V5280
Trifluoroacetic acid (TFA)	Fisher scientific	O4902-100
Critical commercial assays		
ECL Western Blotting reagents	Cytiva	RPN2106
Pierce™ BCA protein assay kit	ThermoScientific	23225
Deposited data		
Proteomics data	MassIVE	MSV000092568
Experimental models: Cell lines		
Neuro 2a	ATCC	CCL-131
Experimental models: Organisms/strains		
Mouse: C57BL/6J	Mice bred in-house	N/A
Oligonucleotides		
eEF1A1 shRNA-resistant Primer – Forward 5′-GTGGTTACCTTTGCTCCGGTCAACGTGACGA CCGAGGTCAAGTCTGTTG-3′	Eurofins	This paper
eEF1A1 shRNA-resistant Primer – Reverse 5′-CAACAGACTTGACCTCGGTCGTCACGTTGAC CGGAGCAAAGGTAACCAC-3′	Eurofins	This paper

(Continued on next page)

Continued

REAGENT or RESOURCE	SOURCE	IDENTIFIER
TUFM shRNA-resistant Primer – Forward 5'-GCCATGCCTGGAGAAGATCTGAAGCTGAGC CTGATCTTGCGGCAGCC-3'	Eurofins	This paper
TUFM shRNA-resistant Primer – Reverse 5'- GGCTGCCGCAAGATCAGGCTCAGCTTCAGA TCTTCTCCAGGCATGGC-3'	Eurofins	This paper
Recombinant DNA		
Non-Target control shRNA - pLKO.1-puro-CMV-TagRFP shRNA sequence - GCGCGATAGCGCTAATAATTT	Sigma-Aldrich	SHC016
V5-tagged mitochondrial targeting sequence – pcDNA3.1-Matrix-Apex-V5/His	Custom made	N/A
TUFM shRNA - pLKO.1-puro-CMV-TagCFP shRNA sequence - GGACTTGAAGCTTAGTCTAAT	Sigma-Aldrich	TRCN0000248733
TUFM WT - pCMV (Myc-DDK-tagged)	OriGene	MR217099
TUFM shRNA-resistant - pCMV (Myc-DDK-tagged)	This paper	N/A
eEF1A1 shRNA - pLKO.1-puro-CMV-TagRFP shRNA sequence - CCAGTCAATGTAACAACTGAA	Sigma-Aldrich	TRCN0000123776
eEF1A1 WT - pCMV (V5-His tagged)	This paper	N/A
eEF1A1 shRNA-resistant - pCMV (V5-His tagged)	This paper	N/A
Software and algorithms		
Prism v9.0.0	Graphpad	https://www.graphpad.com/
Fiji (Image J)	Schindelin et al.[48]	https://imagej.net/software/fiji/
Inkscape 1.0.1	Inkscape	https://inkscape.org/
Other		
Microfluidics 450 μm microgroove barrier	Xona	SND450
Zeiss LSM 710 Confocal microscope	Zeiss	N/A
Zeiss LSM 880 Confocal microscope	Zeiss	N/A
Amersham 680 RGB	GE Healthcare	N/A
Amersham ImageQuant 800	GE Healthcare	N/A
Mini Gel Tank and Blot Module Set	Invitrogen	NW2000
Potter Elvehjem 30mL	Fisher Scientific	10669922
Peptide desalting spin columns	Thermo Fisher Scientific	89882
nanoViper analytical column	Thermo Fisher Scientific	164570
Orbitrap Fusion	Thermo Fisher Scientific	

RESOURCE AVAILABILITY

Lead contact

Further information and requests for resources and reagents should be directed to and will be fulfilled by the lead contact, Vanessa A. Morais (vmorais@medicina.ulisboa.pt).

Materials availability

This study did not generate new unique reagents.

Data and code availability

- All datasets reported in this work are available from the lead contact upon request.
- This paper does not report original code.
- Any additional information required to reanalyse the data reported in this paper is available from the lead contact upon request.

- All data generated or analysed during this study are included in the manuscript and supporting files. RAW MS data has also been deposited at MassIVE under the accession number Database: MSV000092568.

EXPERIMENTAL MODEL AND STUDY PARTICIPANT DETAILS

Animals

C57BL/6J mice were obtained from the Rodent Facility from Instituto de Medicina Molecular – João Lobo Antunes (Lisbon, Portugal), where they were housed in a temperature-controlled room at 20-24°C. Stud males were housed individually. Females were housed in groups of 2-5 per cage and synchronization of their estrous cycles was achieved by exposing them to male's urine 48h prior to mating. Embryos at embryonic day 18 (E18) were used for primary neuron cultures. All the procedures were approved by the Portuguese National Authority for Animal Health (DGAV), as well as by the institute's animals' well-being office (ORBEA-iMM). The study was carried out in compliance with the ARRIVE guidelines.[49]

Cell lines

Mouse neuroblastoma cell lines (N2a) were grown in Dulbecco's Modified Eagle Medium/Nutrient Mixture F-12 (DMEM-F12) supplemented with 10% Fetal Bovine Serum (FBS), at 37°C and 5% CO_2.

METHOD DETAILS

Mouse primary neuronal culture

Mouse primary neuronal cultures were obtained from whole brain of E18 embryonic C57BL/6 mice, as previously described.[34] Whole-brains were collected in Hank's Balanced Salt Solution supplemented with 1M HEPES (HBSS-HEPES). Meninges were removed, and brains were homogenised and dissociated with 0.25% trypsin + 10μl/ml DNaseI in HBSS-HEPES for 15min at 37°C. Tissue was washed with 10% Horse serum (HS) in HBSS-HEPES and centrifuged 1.200xg for 10min at RT. Supernatant was discarded and pellet was washed two more times with HBSS-HEPES. Pellet was resuspended in 10% HS in Minimum Essential Medium (MEM) with 0.6% Glucose and 100U/ml Penicillin-Streptomycin (MEM-HS); and strained using a 70μm cell strainer. Cell viability was assessed using Trypan blue. Cells were plated at $1x10^5$ cells/well on 13mm coverslips (in a 24 well plate) coated with 0.01mg/ml Poly-D-Lysine hydrobromide. After 4h, medium was replaced with Neurobasal medium supplemented 0.5mM L-Glutamine, 20U/ml Penicillin-Streptomycin and 2% B-27 (NB-B27).

For Microfluidic devices,[32,50] standard 2-compartment devices with 450μm microgroove barrier were placed on top of a 24mm coverslip coated with 0.01mg/ml Poly-D-Lysine hydrobromide. Neurons were plated in the somal compartment ($8x10^4$ cells per microfluidic) and maintained in MEM-HS for 4h and then replaced by NB-B27. Fresh NB-B27 was added every 3 days. A volume difference between the somal (170-180μL) and the axonal (120-130μL) compartments was maintained to create a hydrostatic pressure, thus fluidically isolating each compartment.

Labelling mtDNA replication sites using BrdU/EdU

Neurons were treated with 10μM BrdU or 10μM EdU for 4h. As a negative control, neurons were treated either with BrdU or EdU together with 100μM ddC, an inhibitor of mtDNA replication, or DMSO only (solvent control).

For the inhibition of protein translation, neurons were treated with 100μg/mL cycloheximide or 150μg/mL chloramphenicol according to the referred time points.

Labelling nuclear-encoded protein synthesis with puromycin

Neurons were treated with 10μM puromycin for 10min. Nuclear-encoded protein translation was blocked with 100μg/mL cycloheximide for the respective time-points, before adding of puromycin.

Labelling mitochondrial-encoded protein synthesis with HPG

Neurons were placed in a methionine-free medium (HBSS-HEPES) for 30 min and then incubated with 500μM HPG for another 30min. Mitochondrial-encoded protein translation was inhibited with 150μg/mL chloramphenicol and nuclear-encoded protein translation was inhibited with 100μg/mL cycloheximide for 3h, prior to HPG.

Immunofluorescence assay

Neurons were washed in PBS$^{+/+}$ (0.33mM MgCl$_2$.6H$_2$O, 0.9mM CaCl$_2$.2H$_2$O) and fixed in 4% paraformaldehyde (PFA) in PBS$^{+/+}$ for 20min at RT. Neurons were permeabilized with 0.5% Triton X-100 in PBS$^{+/+}$ for 10min at RT and washed with PBS. Blocking was performed for 1h at RT with blocking buffer (0.2% gelatine, 2% FBS, 2% BSA, 0.3% Triton X-100 in PBS) supplemented with 5% goat serum followed by primary antibody incubation overnight at 4°C. Incubation with secondary antibodies conjugated with Alexa-Fluorophores and DAPI (1μg/mL) was performed for 1h at RT. Coverslips were mounted on Vectashield.

For the BrdU protocol, after fixation, DNA was denatured with 1M HCl for 30min at 37°C, washed 3x with 0,1M Boric Acid pH=8,5 for 5min at RT.

For the EdU and HPG protocols, washes were performed in 3%BSA in PBS. After blocking, EdU and HPG were stained using a click-chemistry reaction cocktail (100mM Tris-HCl pH 8.5, 5μM Alexa Fluor 488-Azide, 1mM $CuSO_4$ and 100mM Ascorbic Acid) for 30min at RT.

For microfluidics, neurons were pre-fixed for 5min at 37°C with 5% CO_2, by adding 4% PFA to each compartment (together with NB-B27). Pre-fixation solution was removed, and 4% PFA was added to each compartment for 20min at RT. Each compartment was washed with PBS$^{+/+}$. Microfluidic chamber was carefully removed, and coverslip was washed with PBS$^{+/+}$. Neurons were permeabilized with 0.5% Triton X-100 and immunofluorescence protocol proceeded as mentioned above.

Images were acquired on a Zeiss LSM 880 or a Zeiss LSM 710 confocal microscope with 63x oil objective, numerical aperture (NA) 1.4.

Isolation of synaptic and non-synaptic mitochondria from mouse brain

Brains were isolated from 8 weeks old C57BL/6J female mice and homogenized with a rotating Teflon 30mL Potter-Elvehjem (15-20 strokes, 800rpm) in a cold isolation buffer (IB) containing 10mM HEPES, 225mM sucrose, 75mM D-Mannitol and 1mM EGTA, pH 7.4, followed by centrifugation at 600xg, 10min, 4°C. Supernatant (brain homogenate fraction) was collected and further centrifuged at 15000xg, 10min, 4°C. Pellet (crude mitochondrial fraction) was ressuspended in 15% Percoll and applied on a 40% and 24% Percoll cushion, forming an ascending Percoll gradient (adapted from[51]). Percoll gradient was centrifuged in a fixed rotor at 31,000xg, 9min, 4°C, with maximum acceleration and slow deceleration. Top white phase (mostly myelin) was removed and synaptosomes (in the interphase 15% - 24% Percoll) and non-synaptic mitochondria (in the interphase 24% - 40% Percoll) were collected. Each fraction was ressuspended in cold IB with 4 times the volume of each fraction and suffered sequential centrifugation at 20,000xg and 10,000xg for 10min, 4°C. In order to collect the synaptic mitochondria, synaptosomes were disrupted with 0,6mg/mL of digitonin (diluted in IB) for 15min, 4°C, followed by two centrifugations at 10,000xg, 10min, 4°C.

Proteomics

The stable ^{15}N isotope labelling of mammals was accomplished essentially as previously described.[52,53] Briefly, FVB mice of both sexes were purchased immediately after weaning. After a week-long acclimation, mice were placed on *ad libitum* ^{15}N diet (MF-SpirulinaN-IR; Cambridge Isotopes). For the dynamic labelling experiments (single-generation), mice stayed on the 15N diet for 4 months and were sacrificed. Mice were anesthetized with 3% isoflurane followed by acute decapitation. Brain tissues were harvested, flash frozen in a dry ice/ethanol bath, and stored at −80°C.

For consequent MS studies, brain homogenates from naturally occurring N14 fresh brains from C57BL/6J female mice were mixed in a 1:1 ratio with brain homogenates coming from N15 labelled frozen brains. From the N14/N15 mixed brain homogenate, mitochondria were isolated as described above.

MS sample preparation

Mitochondrial samples were homogenized in the lysis buffer (0.1 M Tris-HCl, pH 7.6, 20% SDS and 1 M DTT with 1✕ protease inhibitor cocktail.[54] The mixtures were incubated at 95°C for 5 min. The samples were then sonicated for 10 min and centrifuged at 16,100 x g for 10 min. The supernatant was collected and the proteins were precipitated by the methanol/chloroform method. Protein pellets were resuspended in 8 M urea prepared in 100 mM ammonium bicarbonate solution and processed with ProteaseMAX according to the manufacturer's protocol. The samples were reduced with 5 mM Tris(2-carboxyethyl)phosphine (TCEP; vortexed for 1 hour at RT), alkylated in the dark with 10 mM iodoacetamide (IAA; 20 min at RT), diluted with 100 mM ABC, and quenched with 25 mM TCEP. Samples were diluted with 100 mM ammonium bicarbonate solution, and digested with Trypsin (1:50,) for overnight incubation at 37°C with intensive agitation. The next day, reaction was quenched by adding 1% trifluoroacetic acid (TFA). The samples were desalted using Peptide Desalting Spin Columns. All samples were vacuum centrifuged to dry.

Tandem mass spectrometry

Three micrograms of each sample were auto-sampler loaded with a Thermo EASY nLC 100 UPLC pump onto a vented Acclaim Pepmap 100, 75 um x 2 cm, nanoViper trap column coupled to a nanoViper analytical column (3 μm, 100 Å, C18, 0.075 mm, 500 mm) with stainless steel emitter tip assembled on the Nanospray Flex Ion Source with a spray voltage of 2000 V. An Orbitrap Fusion was used to acquire all the MS spectral data. Buffer A contained 94.785% H2O with 5% ACN and 0.125% FA, and buffer B contained 99.875% ACN with 0.125% FA. The chromatographic run was for 4 hours in total with the following profile: 0-7% for 7, 10% for 6, 25% for 160, 33% for 40, 50% for 7, 95% for 5 and again 95% for 15 mins receptively. Samples were injected and analyzed by three or six times.

We used CID-MS2 method for these experiments as previously described.[55] Briefly, ion transfer tube temp = 300°C, Easy-IC internal mass calibration, default charge state = 2 and cycle time = 3 s. Detector type set to Orbitrap, with 60K resolution, with wide quad isolation, mass range = normal, scan range = 300-1500 m/z, max injection time = 50 ms, AGC target = 200,000, microscans = 1, S-lens RF level = 60, without source fragmentation, and datatype = positive and centroid. MIPS was set as on, included charge states = 2-6 (reject unassigned). Dynamic exclusion enabled with n = 1 for 30 s and 45 s exclusion duration at 10 ppm for high and low. Precursor selection decision = most intense, top 20, isolation window = 1.6, scan range = auto normal, first mass = 110, collision energy 30%, CID, Detector type = ion trap, OT resolution = 30K, IT scan rate = rapid, max injection time = 75 ms, AGC target = 10,000, Q = 0.25, inject ions for all available parallelizable time.

MS data analysis and quantification

Protein identification/quantification and analysis were performed with Integrated Proteomics Pipeline - IP2 (Bruker, Madison, WI. http://www.integratedproteomics.com/) using ProLuCID,[56,57] DTASelect2,[58,59] Census and Quantitative Analysis. Spectrum raw files were extracted into MS1, MS2 files using RawConverter (http://fields.scripps.edu/downloads.php). The tandem mass spectra (raw files from the same sample were searched together) were searched against UniProt mouse (downloaded on 03-25-2014) protein databases[60] and matched to sequences using the ProLuCID/SEQUEST algorithm (ProLuCID version 3.1) with 50 ppm peptide mass tolerance for precursor ions and 600 ppm for fragment ions. The search space included all fully and half-tryptic peptide candidates within the mass tolerance window with no-miscleavage constraint, assembled, and filtered with DTASelect2 through IP2. To estimate protein probabilities and false-discovery rates (FDR) accurately, we used a target/decoy database containing the reversed sequences of all the proteins appended to the target database.[60] Each protein identified was required to have a minimum of one peptide of minimal length of six amino acid residues; however, this peptide had to be an excellent match with an FDR < 1% and at least one excellent peptide match. After the peptide/spectrum matches were filtered, we estimated that the protein FDRs were $\leq$ 1% for each sample analysis. Resulting protein lists include subset proteins to allow for consideration of all possible protein forms implicated by at least two given peptides identified from the complex protein mixtures. Then, we used Census and Quantitative Analysis in IP2 for protein quantification. Static modification: 57.02146 C for carbamidomethylation. Quantification was performed by the built-in module in IP2.

Transfection of mouse primary neurons

For the loss and gain of function assays, mouse primary neurons at DIV4-5 were transfected using the calcium phosphate method and incubated with EdU and fixed at DIV7. Coverslips were transferred to a new plate containing NB-B27 supplemented with 2mM kynurenic acid (KA). For each well, 1.5μg of total DNA was diluted in 17.5μL TE buffer (10 mM Tris, 1 mM EDTA, pH 7.3). CaCl$_2$ solution (2.5M in 10mM HEPES, pH 7.2) was added dropwise to the diluted DNA (final concentration = 250 mM CaCl2) and gently mixed. This mix was then added dropwise to an equivalent volume of HEPES-buffered saline (274mM NaCl, 10mM KCl, 1.4mM Na$_2$HPO$_4$, 11mM glucose, 42mM HEPES, pH 7.2), gently mixed and incubated at RT for 30min. Transfection mix was added dropwise to neurons, followed by an incubation of 3h at 37°C with 5% CO$_2$. Finally, neurons were washed with acidified medium (NB (without B27) supplemented with 2mM kynurenic acid and ~5mM HCl) for 15min at 37°C with 5% CO$_2$. Coverslips were transferred to the original plates (with conditioned neuronal culture media) and maintained in the incubator (37°C with 5% CO$_2$).

Transfection of N2a

N2a were transfected in 6 well plate, using Lipofectamine 2000 at a ratio of DNA/Lipofectamine of 1:2 (4μg of DNA:8μL of Lipofectamine per well). Cells were transfected in serum-free DMEM-F12 for 4h. After transfection, the medium was replaced by fresh DMEM-F12 supplemented with 10% FBS. N2a were lysed 48h after transfection.

Cell lysis and immunoblot

N2a cells were lysed with Lysis buffer (50mM Tris-HCl, pH7.4, 5mM EDTA, 150mM NaCl, 1% Triton X-100) supplemented with Protease inhibitors for 1h at 4°C. After lysis, cells were centrifuged at 300 xg for 10min at 4°C, supernatant was collected, and protein concentration was quantified using Pierce™ BCA Protein Assay Kit.

For immunoblot analysis, equal amount of protein extracts (5-20 μg/well) were separated by SDS-PAGE (Invitrogen) in MOPS-SDS running buffer and transferred onto 0.2μm nitrocellulose membranes for 1h at 30V. Membranes were blocked with 5% milk in TBS-T (20mM Tris-HCl pH7.5, 150mM NaCl, 0.5% Tween-20) for 1h. Primary antibody incubations were performed overnight at 4°C. Washes were performed for 5min at RT in TBS-T. Incubation with Horseradish peroxidase (HRP) conjugated secondary antibodies was performed for 2h at RT. Detection was done using the chemiluminescent ECL-Plus detection kit (Amersham) on a digital Amersham Imager 680 or 800 (GE Healthcare). See also Table S1.

QUANTIFICATION AND STATISTICAL ANALYSIS

Image analysis and quantification

Microscopic images were analysed using Fiji (ImageJ). After maximum intensity projection, a region of interest (ROI) of the neuron to analyse was defined manually. We set a threshold for BrdU/EdU and a threshold for mitochondria (Citrate Synthase or HSP60) and converted the images into binary. For each N, the exact same threshold was applied for BrdU/EdU channel among the different conditions. Mitochondrial threshold was set automatically using Otsu. BrdU/EdU co-localizing with mitochondria was obtained by multiplying BrdU/EdU by mitochondria. We determined the total area of BrdU/EdU; the total area of mitochondria and the area of BrdU/EdU co-localizing with mitochondria. For each neuron, the mitochondrial replication rate was then obtained by normalizing the area of BrdU/EdU co-localizing with mitochondria by the area of mitochondria.

In transfected neurons, ROI of the neuron to analyse was defined automatically based on the signal from the tagged shRNA. For compartmentalized analysis (somal vs. periphery), we defined a ROI for the somal part and the data outside that somal ROI was considered as periphery. Total quantification resulted from the sum of the somal and periphery quantifications.

Statistical analysis

Data distribution was assessed using a boxplot where a visual indication of data set's 25th percentile, 75th percentile, median (or 50th percentile) and individual values are spread out and compared to each other. For all the quantitative analysis, at least 3 independent experiments based on 3 different primary neuron cultures were performed. The statistical analysis was implemented using Prism 9.0.0 software (GraphPad). An appropriate statistical test was chosen based on the dataset. The detailed information is provided in each figure legend.